



DEVELOPMENT OF FUEL-FLEXIBLE GAS TURBINE COMBUSTOR

Tomohiro Asai, Ph.D.

Research Manager
Mitsubishi Hitachi Power Systems, Ltd.
Hitachinaka-shi, Ibaraki, Japan

Yasuhiro Akiyama

Research Staff Member
Mitsubishi Hitachi Power Systems, Ltd.
Hitachinaka-shi, Ibaraki, Japan

Keita Yunoki

Researcher
Mitsubishi Hitachi Power Systems, Ltd.
Hitachinaka-shi, Ibaraki, Japan

Nobuyuki Horii

General Manager
Mitsubishi Hitachi Power Systems, Ltd.
Hitachi-shi, Ibaraki, Japan

Keisuke Miura

Research Manager
Mitsubishi Hitachi Power Systems, Ltd.
Hitachinaka-shi, Ibaraki, Japan

Mitsuhiro Karishuku

Engineering Manager
Mitsubishi Hitachi Power Systems, Ltd.
Hitachi-shi, Ibaraki, Japan

Satoschi Dodo

Engineering Manager
Mitsubishi Hitachi Power Systems, Ltd.
Hitachi-shi, Ibaraki, Japan



Dr. Tomohiro Asai is a research manager in the Thermal Power Systems Research Department, Research and Development Center, Mitsubishi Hitachi Power Systems, Ltd., Japan (MHPS). Dr. Asai joined Hitachi, Ltd. in 2002 and was transferred to MHPS in 2014. He has been working on the research and development of combustors for fuel flexible gas turbines for over ten years, focusing on hydrogen content gaseous fuels and low-grade oil fuels. He has authored or coauthored fifteen technical papers on gas turbine combustion technology and holds six patents. In 2011, he was awarded the Gas Turbine Society of Japan (GTSJ) Prize for the new technology entitled “Low NO_x Combustion Technology with Multiple-Injection Burners for Hydrogen-Rich Fuels.” He received his master’s degree in 1999 and his Ph.D. in 2003 in aerospace engineering from Osaka Prefecture University, Japan. He is a member of the Japan Society of Mechanical Engineers (JSME), and the GTSJ.



Mr. Keisuke Miura is a research manager in the Thermal Power Systems Research Department, Research and Development Center, Mitsubishi Hitachi Power Systems, Ltd., Japan (MHPS). Mr. Miura joined Hitachi, Ltd. in 2002 and was transferred to MHPS in 2014. He has been working on the research and development of dry low NO_x gas turbine combustors for natural gas over ten years. He has authored or coauthored four technical papers on gas turbine combustion technology and holds eleven patents. In 2014, he was awarded the Combustion Society of Japan Prize for the paper entitled “Large Eddy Simulation of Coaxial Jet Cluster Burner for Gas Turbine Combustor.” He received his bachelor’s degree in 2000 in engineering sciences and his master’s degree in 2002 in systems and information engineering from the University of Tsukuba, Japan. He is a member of the Gas Turbine Society of Japan (GTSJ).



Mr. Yasuhiro Akiyama is a member of the research staff in the Thermal Power Systems Research Department, Research and Development Center, Mitsubishi Hitachi Power Systems, Ltd., Japan (MHPS). Mr. Akiyama joined Hitachi, Ltd. in 2011 and was transferred to MHPS in 2014. He has been working on the research and development of dry low NO_x gas turbine combustors for five years. He has authored or coauthored seven technical papers on gas turbine combustion technology and holds one patent. He received his bachelor’s degree in 2009 and his master’s degree in 2011 in energy sciences from Tokyo Institute of Technology, Japan. He is a member of the Japan Society of Mechanical Engineers (JSME), the Combustion Society of Japan, and the Gas Turbine Society of Japan (GTSJ).



45TH TURBOMACHINERY & 32ND PUMP SYMPOSIA
HOUSTON, TEXAS | SEPTEMBER 12 – 15, 2016
GEORGE R. BROWN CONVENTION CENTER



Mr. Mitsuhiro Karishuku is an engineering manager in the Hitachi Gas Turbine Engineering Department, Gas Turbine Technology & Products Integration Division, Mitsubishi Hitachi Power Systems, Ltd., Japan (MHPS). Mr. Karishuku joined Hitachi, Ltd. in 2008 and was transferred to MHPS in 2014. He has been working on the development design of gas turbines and combustors for eight years. He has coauthored seven technical papers on gas turbine combustion technology and holds one patent. He graduated from the National Institute of Technology, Ichinoseki College, Japan in 1998.



Mr. Keita Yunoki is a researcher in the Thermal Power Systems Research Department, Research and Development Center, Mitsubishi Hitachi Power Systems, Ltd., Japan (MHPS). Mr. Yunoki joined Hitachi, Ltd. in 2010 and was transferred to MHPS in 2014. He has been working on the research and development of numerical simulation technology for gas turbine combustors over five years. He has authored three technical papers on numerical simulation technology and holds one patent. In 2014, he was awarded the Combustion Society of Japan Prize for the paper entitled "Large Eddy Simulation of Coaxial Jet Cluster Burner for Gas Turbine Combustor." He received his bachelor's degree in 2008 and his master's degree in 2010 in chemical engineering from Kyushu University, Japan. He is a member of the Combustion Society of Japan.



Mr. Satoschi Dodo is an engineering manager in the Hitachi Gas Turbine Engineering Department, Gas Turbine Technology & Products Integration Division, Mitsubishi Hitachi Power Systems, Ltd., Japan (MHPS). Mr. Dodo joined Hitachi, Ltd. in 1994 and was transferred to MHPS in 2014. He has been working on the research and development of fuel-flexible gas turbine combustors and distributed power systems for over twenty years. He has authored or coauthored thirteen technical papers on gas turbine combustion technology and holds six patents. In 2011, he was awarded the Gas Turbine Society of Japan (GTSJ) Prize for the new technology entitled "Low NO_x Combustion Technology with Multiple-Injection Burners for Hydrogen-Rich Fuels." He received his master's degree in 1991 in mechanical engineering from the University of Tokyo, Japan and graduated from the doctoral program of the graduate school of engineering, the University of Tokyo in 1994. He is a member of the GTSJ.



Mr. Nobuyuki Horii is currently the general manager of the Hitachi Gas Turbine Engineering Department, Gas Turbine Technology & Products Integration Division, Mitsubishi Hitachi Power Systems, Ltd. (MHPS) in Hitachi, Japan. Mr. Horii joined Hitachi, Ltd. in 1992 and was transferred to MHPS in 2014. He has 24 years of experience in axial flow compressor and turbine design, application engineering, auxiliary system design, functional safety engineering, and project management. He is now the team leader for gas turbine mechanical drive application of both core engine design and package design. He received a B.S. degree in aerospace system engineering from Tokyo Metropolitan Institute of Technology in 1992.

ABSTRACT

Growing global energy demands are motivating the gas turbine industry to seek fuel-flexible gas turbines capable of burning a wide variety of fuels as a means of increasing energy supply stability and security. These fuel-flexible gas turbines require diluent-free ("dry"), low nitrogen oxide (NO_x) and flashback-resistant combustors for various fuels in order to achieve low NO_x emissions and high plant efficiency for low carbon dioxide (CO₂) emissions. This paper describes the development of a state-of-the-art dry low-NO_x and flashback-resistant combustor for fuel-flexible gas turbines.

This advanced combustor consists of multiple fuel nozzles and multiple air holes. One fuel nozzle and one air hole are installed coaxially to give one key element, and a cluster of key elements constitutes one burner, which forms one flame. Multiple cluster burners constitute a can combustor, and several can combustors are installed on a gas turbine. In this paper, the burner is called a "cluster burner," and the combustor is called a "multi-cluster combustor." The essence of the burner concept is the integration of two key technologies: low-NO_x combustion due to the enhancement of fuel-air mixing; and flashback-resistant combustion due to short premixing sections, air-stream-surrounded fuel jets and lifted flames.



The development approach of the multi-cluster combustor consists of three steps: burner development; combustor development; and feasibility demonstration for practical plants. The first step optimizes burner configurations by fundamental research at atmospheric pressure. The second step optimizes combustor configurations by single-can combustor testing at medium to high pressures. The third step demonstrates the feasibility of the combustor by field testing with real gas turbines.

This paper describes the development work in each step of the multi-cluster combustor developed particularly for hydrogen content syngas fuels in a coal-based integrated gasification combined cycle (IGCC), and the field test in an IGCC pilot plant demonstrates the feasibility of the combustor for practical plants. This paper also describes applications of this combustion technology to expand fuel flexibility.

INTRODUCTION

Growing global energy demands are motivating the gas turbine industry to seek fuel-flexible gas turbines capable of burning a wide variety of fuels as a means of increasing energy supply stability and security. These fuel-flexible gas turbines must achieve low NO_x emissions and high plant efficiency with the various fuels in order to cut CO₂ emissions. Figure 1 plots available gaseous fuels for fuel-flexible gas turbines in a graph showing the relationship between the Wobbe index, which is defined as the lower heating value divided by the square root of the fuel specific gravity, and the normalized laminar flame speed. The available fuels cover a wide range of Wobbe indices from those of hydrogen (H₂) content syngas produced in the IGCC with CO₂ capture and storage (CCS) systems to that of propane, and a wide range of flame speeds from that of natural gas to those of high H₂ content fuels. The H₂ content fuels, dimethyl ether (DME), and propane possess higher flame speeds than that of natural gas. Figure 2 plots the available fuels in terms of H₂ contents in each fuel type and lower heating values per volume. The available fuels cover a wide range of H₂ contents, and they also satisfy energy needs of the oil and gas industry and the petrochemical industry.

Conventional gas turbine combustors are incapable of achieving low-NO_x, flashback-resistant combustion, and high plant efficiency for fuel-flexible gas turbines. Figure 3 summarizes technical hurdles with conventional combustors. They are broadly classified into two types: a premixed combustor and a diffusion-flame combustor. Conventional premixed combustors are capable of achieving low NO_x combustion by supplying a premixed fuel-air mixture because they maintain low local flame temperatures. However, premixed combustors burning a wide variety of fuels are prone to flashback into their large premixing section because they are highly tuned to operate on low-flame-speed fuels like natural gas. The flashback tendency characteristic hinders the application of premixed combustion technology to a wide variety of fuels for fuel-flexible gas turbines. In contrast, conventional diffusion-flame combustors are capable of achieving flashback-resistant combustion of a wide variety of fuels by supplying fuel and air separately into their combustion chamber. However, diffusion-flame combustors are incapable of achieving high plant efficiency because they require the additional energy to inject a diluent, such as water, steam, or nitrogen, into the combustion zone in order to suppress the increased NO_x emissions due to its high local flame temperatures. The practical fuel-flexible gas turbines have so far employed diffusion-flame combustors at the expense of the decreased plant efficiency in order to achieve flashback-resistant combustion of a wide variety of fuels.

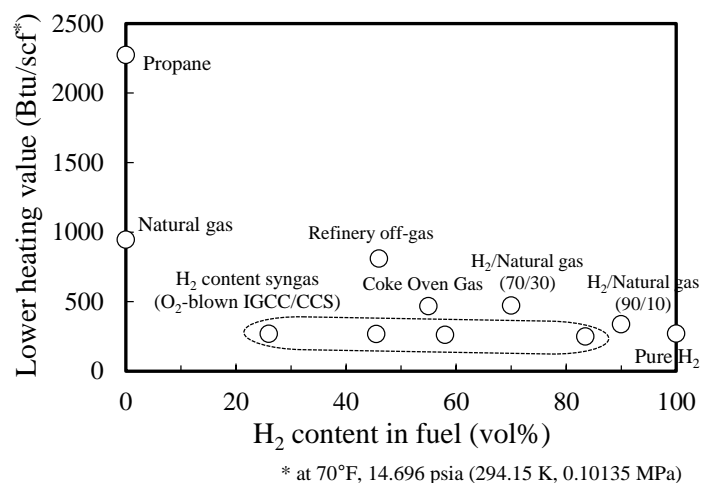
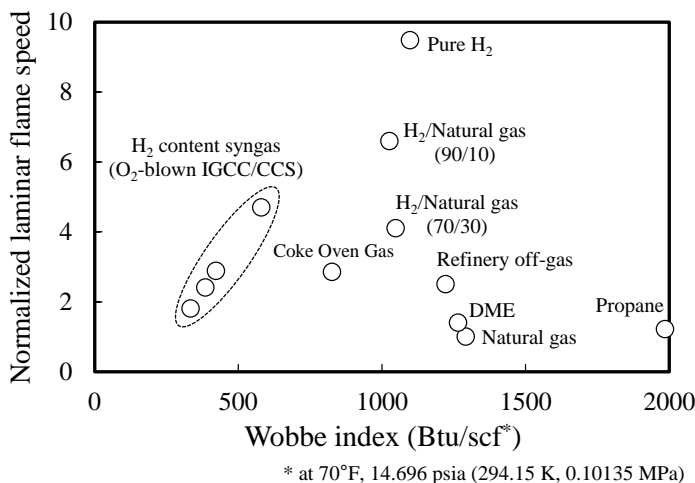


Figure 1. Available Gaseous Fuels for Fuel-Flexible Gas Turbines (Laminar Flame Speed versus Wobbe Index)

Figure 2. Available Gaseous Fuels for Fuel-Flexible Gas Turbines (Lower Heating Value versus H₂ Content in Fuel)



A solution to these hurdles is to develop state-of-the-art technologies for diluent-free (“dry”), low-NO_x and flashback-resistant combustion of a wide variety of fuels for fuel-flexible gas turbines. Figure 4 compares merits of dry low-NO_x (DLN) combustors with those of conventional diffusion-flame combustors. Diffusion-flame combustors decrease NO_x by injecting diluents. This method is called “wet control.” However, injection of diluents decreases plant efficiency. In contrast, dry low-NO_x combustors achieve low-NO_x diluent-free (dry), thereby increasing plant efficiency. This paper describes the development of an advanced DLN and flashback-resistant combustor.

| Combustor type | Premixed combustor | Diffusion-flame combustor |
|---------------------------------|---------------------|--|
| | | |
| Merit | Low NO _x | Flashback-resistant |
| Demerit | Flashback-prone | Plant efficiency decrease (due to diluents injection for NO _x decrease) |
| Experience for fuel-flexible GT | No | Yes |

Figure 3. Technical Hurdles with Conventional Combustors

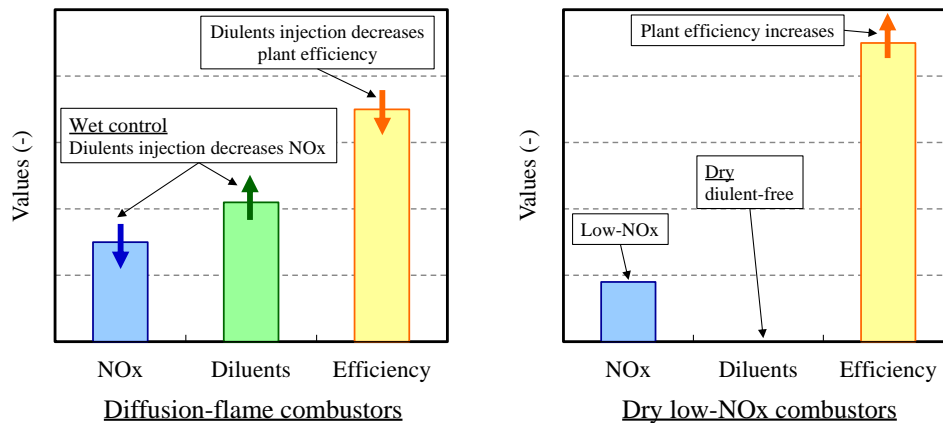


Figure 4. Merit of Dry Low-NO_x Combustors

DEVELOPMENT APPROACH

Figure 5 shows the development approach for the advanced DLN and flashback-resistant combustor. The development approach consists of three steps: burner development; combustor development; and feasibility demonstration for practical plants.

In Step 1, the purpose is to optimize configurations of single burners with pairs of a fuel nozzle and an air hole by performing a single-nozzle mixing test and a single-burner combustion test at atmospheric pressure. Step 1 evaluates performance of single burners in terms of emissions of NO_x, carbon monoxide (CO) and unburned hydrocarbons (UHC), and stability, which is related to pressure fluctuations due to combustion oscillation.

In Step 2, the purpose is to optimize configurations of single-can combustors by a single-can combustion test at medium and high pressures on the basis on the burner configurations optimized in Step 1. Step 2 evaluates performance of single-can combustors in terms of emissions, stability, and reliability, which is related to metal temperatures of burners and combustion liners.

In Step 3, the purpose is to demonstrate combustor performance in practical plants by a real gas turbine test in a multi-can configuration at a practical pressure. Step 3 evaluates performance of multi-can combustors in terms of emissions, stability, reliability, and operability, which is related to dynamic characteristics of the combustors during their operation.

| | Step 1 | Step 2 | Step 3 |
|---------------|--|--|---|
| | Burner development | Combustor development | Feasibility demonstration for practical plants |
| Action | Optimization of burner configurations | Optimization of combustor configurations | Demonstration of combustor performance in practical plants |
| Configuration | - Pair of a fuel nozzle and an air hole - Single burner | Single-can combustor | Multi-can combustors |
| Pressure | Atmospheric pressure | Medium and high pressures | Practical pressure |
| Test | - Single-nozzle mixing test - Single-burner combustion test | Single-can combustion test | Real gas turbine test in multi-can configuration |
| Evaluation | - Emissions (NO _x , CO, UHC) - Stability (Pressure fluctuations) | - Emissions (NO _x , CO, UHC) - Stability (Pressure fluctuations) - Reliability (Metal temperatures) | - Emissions (NO _x , CO, UHC) - Stability (Pressure fluctuations) - Reliability (Metal temperatures) - Operability (Dynamic characteristics) |

Figure 5. Development Approach for the Advanced DLN and Flashback-Resistant Combustor

AN ADVANCED DLN AND FLASHBACK-RESISTANT COMBUSTOR

Combustor Configuration

Figure 6 shows the configuration of the advanced DLN and flashback-resistant combustor. The combustor consists of multiple fuel nozzles and multiple air holes. The key elements of the combustor each consist of one fuel nozzle and one air hole that are installed coaxially. A cluster of key elements constitutes one burner, which forms one flame. The air holes are embedded in one plate. Multiple cluster burners constitute a can combustor, and several can combustors are installed on a gas turbine. Hereafter, this burner is called a “cluster burner,” and this combustor is called a “multi-cluster combustor.”

The multi-cluster combustor shown in Figure 6 is equipped with a pilot burner at the center and six identical main burners surrounding the pilot burner. The combustor forms seven individual flames, each of which is anchored to the corresponding burner. The combustor assigns operational stability to the pilot burner and low-NO_x operation to the main burners. The pilot burner increases combustion stability over the entire operating range by generating a well-stabilized flame in the center region of the combustion chamber. The main burners achieve low-NO_x combustion by mixing fuel and air homogeneously. The combustor can be used for dual-fuel operation with gaseous fuel and oil fuel. The combustor operates on gaseous fuel for the burners and on oil fuel by using an air-assisted oil spray nozzle installed at the center of the pilot burner.

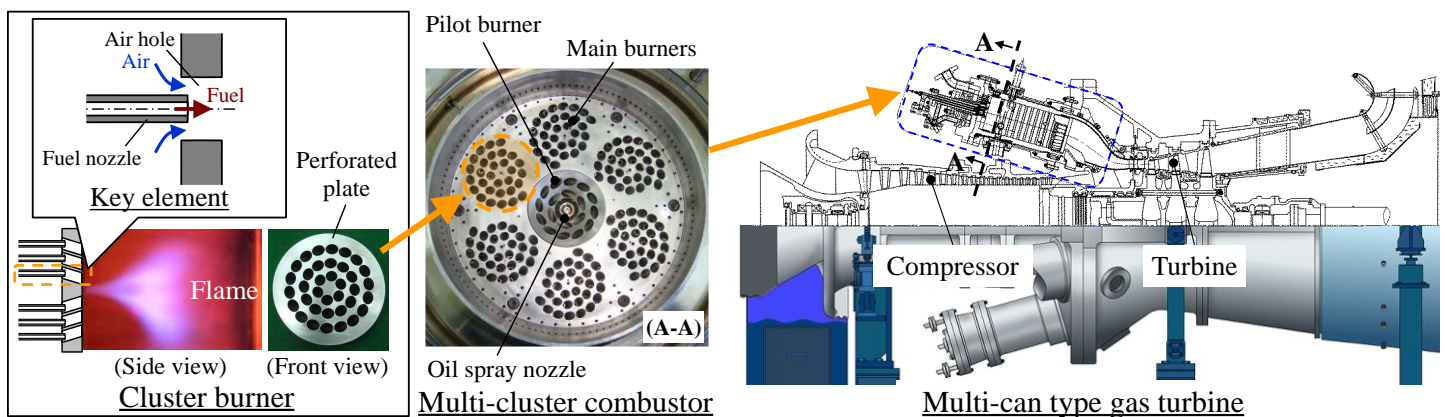


Figure 6. Configuration of the Advanced DLN and Flashback-Resistant Combustor



Burner Concept

The concept of the cluster burner is based on the integration of two key technologies: low-NO_x combustion and flashback-resistant combustion. The cluster burner provides both the premixed combustor’s advantage of low-NO_x combustion and the diffusion-flame combustor’s advantage of flashback-resistant combustion. Figure 7 illustrates the concept.

The burner achieves low-NO_x combustion by mixing fuel and air rapidly and dispersing fuel with multiple fuel-air coaxial jets. Each coaxial jet in a single air hole is comprised of a central fuel jet surrounded by an annular air stream. The coaxial jet generates turbulence through the abruptly-expanding flow just downstream from the exit of the air hole. The turbulence increases the amplitude of a wave-like disturbance at the boundary between fuel and air streams just downstream from the exit, thus mixing fuel and air rapidly. Moreover, the burner disperses fuel by multiplying the coaxial jet, thereby enhancing fuel-air mixing. Homogeneous mixing achieves low-NO_x combustion by eliminating high-temperature and NO_x-generating regions.

The burner achieves flashback-resistant combustion due to the following three effects: a short premixing section; an air-stream-surrounded fuel jet; and a lifted flame. First, the short premixing section of the air hole decreases the risk of flashback. The short premixing section serves as a space free from flame anchoring points. In addition, the short premixing section decreases the risk of autoignition of a fuel-air mixture in the section because the residence time of the fuel-air mixture there is shorter than the ignition delay time. Second, a fuel jet surrounded by an annular air stream decreases the risk of flashback. The air-stream-surrounded fuel jet provides the fuel-air mixture outside the flammable range in the air hole, thus preventing flames from propagating upstream into the air hole. Third, the lifted flame decreases the risk of flashback because the lifted flame is held stably at a point away from the burner.

Figure 8 shows a cross-sectional view of the cluster burner to illustrate the operating principle of the flame-lifting technology. The burner lifts a flame by producing converging and diverging swirl flows just downstream from itself. The air holes cause the combustion air passing through them to swirl because the central axis of each hole is inclined in the direction of a tangent to each circle of holes. The swirling flow emanating from the air holes first converges towards, and then diverges from, an axial position (i.e., the flame anchoring point), which is located away from the burner. The converging-diverging swirl flows induce a pressure profile in the flow direction as shown in the figure. The converging swirl flow induces a favorable pressure gradient because of the decrease in pressure downstream with increasing swirl velocity, whereas the diverging swirl flow induces an adverse pressure gradient because of the increase in pressure downstream with decreasing swirl velocity. The adverse pressure gradient causes a vortex breakdown at the boundary between the converging and the diverging swirl flows, thereby producing a recirculation flow in the diverging swirl flow. The recirculation flow stabilizes the flame by providing a stable heat source of combustion gas for continuous ignition of the fresh reactants. The reverse flow of the combustion gas and the vortex breakdown bubble from the boundary can be suppressed by the favorable pressure gradient in the converging swirl flow. Consequently, the flame is stabilized at the flame anchoring point on the boundary. According to this operating principle, the flame is lifted from the burner. The lifted flames are effective in decreasing the risk of flashback into the burner, especially in H₂ content fueled combustion.

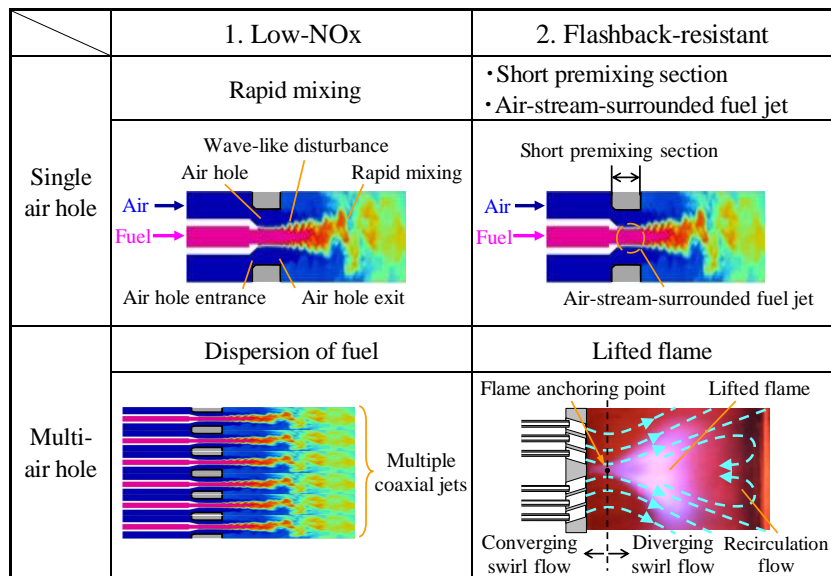


Figure 7. Burner Concept



The cluster burner is capable of controlling combustion by distributing fuel to multiple circuits. The burner arranges injection points in three circles: the first circle with the smallest diameter, the second circle with the middle diameter, and the third circle with the largest diameter (Figure 9). From now on, the region within the first circle on the perforated plate is referred to as an “inner region,” and the region outside the first circle is referred to as an “outer region.” The gaseous fuel injected from fuel nozzles on the first circle is referred to as “inner fuel,” and the gaseous fuel injected from fuel nozzles on the second and third circles is referred to as “outer fuel.” The distribution ratio of the inner and outer fuels affects combustion performance: that is, combustion stability and low-NO_x combustion performance. The increase in the inner-fuel distribution ratio can increase combustion stability, whereas the increase in the outer-fuel distribution ratio can suppress NO_x emissions. A mixture of the inner fuel and air passing through the air holes on the first circle is related to flame stabilization, because the mixture delivers fresh reactants directly to the flame anchoring point. In contrast, a mixture of the outer fuel and air passing through the air holes on the second and third circles is related to low-NO_x combustion because the mixture is probably more homogeneous owing to the increased mixing length from the burner to the flame front. The control of the fuel distribution allows the burner to adapt to a wide range of operating conditions and a wide variety of fuels. The ratio of the mass flowrate of the outer fuel to that of all the fuel supplied to the burner is referred to as an “outer-fuel ratio” here.

The main burners of the multi-cluster combustor arrange their air holes asymmetrically to strengthen their combustion stability. Figure 10 illustrates the mechanism. The swirling flows from the pilot burner and the main burners rotate in the opposite direction. The asymmetric air hole arrangement generates combustion gas paths from the pilot burner to the main burners. The combustion gas entrained in the main burners increases gas temperatures in them, thus strengthening their combustion stability.

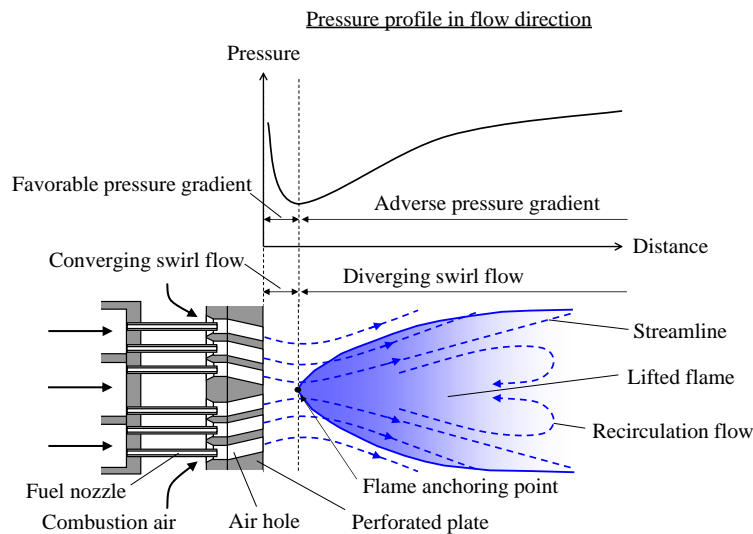
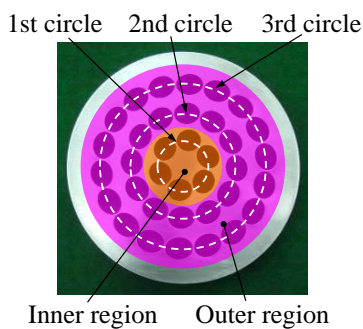


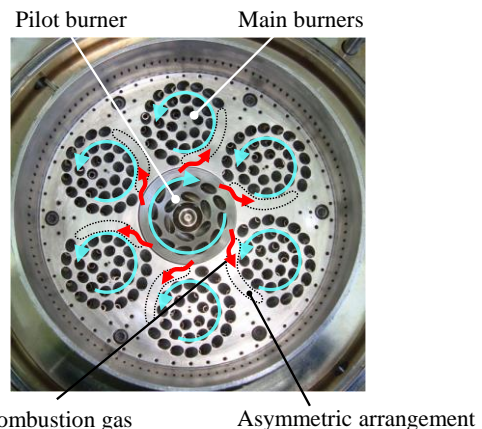
Figure 8. Operating Principle of Flame-Lifting Technology (Courtesy Asai, et al., 2010, ASME)



$$\text{Outer - fuel ratio (\%)} = \frac{Gf_{\text{outer}}}{Gf_{\text{inner}} + Gf_{\text{outer}}}$$

(Gf: mass flowrate, *inner*: inner fuel, *outer*: outer fuel)

Figure 9. Fuel Distribution for Cluster Burner



Combustion gas Asymmetric arrangement from the pilot to the main burners

Figure 10. Asymmetric Arrangement of Air Holes



DEVELOPMENT WORK

The multi-cluster combustor is especially suitable for hydrogen content fuels because the combustor is capable of operating without risk of flashback even for fuels with high flame speeds. This section describes the development work for the multi-cluster combustor intended for hydrogen content syngas fuels in CCS-equipped IGCC plants.

Step 1: Burner Development

Step 1 (burner development) requires development of key fundamental technologies in order to optimize burner configurations. Table 1 summarizes these technologies. Key technology No.1, fuel-air mixing, significantly affects NO_x performance. Step 1 examines the mixing of gaseous fuel and air by using liquid flow to simulate the mixing process of a pair of a fuel nozzle and an air hole that are installed coaxially. Key technology No.2, flame lifting, is effective in decreasing the risk of flashback. For key technology No.3, combustion oscillation is a main topic for modern gas turbine combustors. Combustion oscillation is characterized by large amplitude pressure fluctuations that are driven by unsteady heat release. This oscillation may lead to serious damage of combustor components. Hence, suppression of combustion oscillation is a basic requirement of all combustors (Lieuwen 2012, Lieuwen and Yang 2005, Lieuwen, et al. 2009). Step 1 examines them by a single-burner combustion test at atmospheric pressure.

Table 1. Key Fundamental Technologies for Burner Development

| No. | Key technologies | Evaluation test |
|-----|--|--|
| 1 | Fuel-air mixing in a pair of a fuel nozzle and an air hole | Single-nozzle mixing test |
| 2 | Flame lifting | Atmospheric pressure single-burner combustion test |
| 3 | Suppression of combustion oscillation | |

Single-Nozzle Mixing Test

In the mixing test, milk and water flowed to simulate gaseous fuel and air, respectively. Figure 11 shows a schematic diagram of the single-nozzle mixing test facility. One pair of a fuel nozzle and an air hole was installed in a cylindrical acrylic flow duct. The dimensions of the fuel nozzle and the air hole, and water flow velocity were set to yield the same Reynolds numbers as those for practical burner flows. The laser sheet method based on Mie scattering was employed to visualize the mixing process. Milk functioned as a tracer for the laser diagnostics. The laser used for the test was an argon ion laser with a wavelength of 514.4 nm and an output of 600 mW.

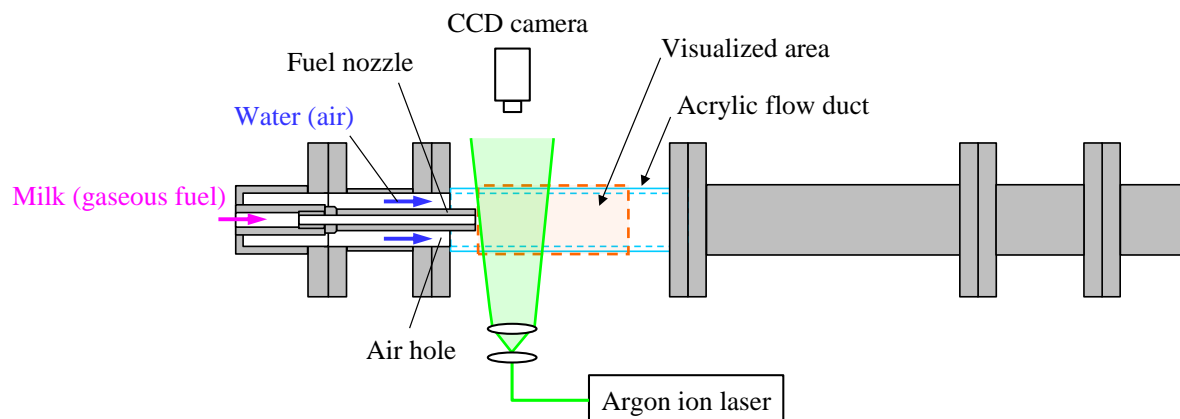


Figure 11. Single-Nozzle Mixing Test Facility

Figure 12 compares the visualized mixing process for a one-direct-hole fuel nozzle and a four-side-hole fuel nozzle. Both fuel nozzles were equipped with a rib at their tip. The one-direct-hole fuel nozzle injected fuel directly into the flow duct in the direction parallel to the air flow. The fuel region remained downstream from the nozzle tip, and then mixed with air gradually due to turbulence generated by the rib. The four-side-hole fuel nozzle injected fuel from the four side holes in the direction perpendicular to the air flow. The fuel mixed with air rapidly upstream from the nozzle tip by impinging the air flow perpendicularly, thereby generating homogeneous fuel-air mixture at the nozzle tip. Hence, the cluster burner is capable of controlling fuel-air mixing by changing fuel nozzle configurations depending on the fuels.

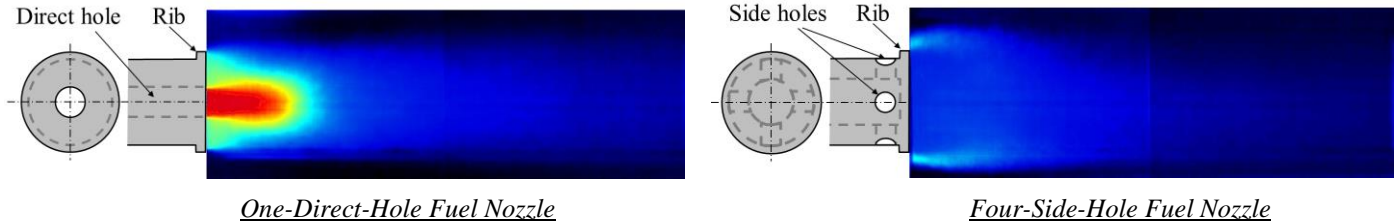


Figure 12. Comparison of Visualized Mixing Process between One-Direct-Hole and Four-Side-Hole Fuel Nozzles

Atmospheric Pressure Single-Burner Combustion Test

The single-burner combustion test at atmospheric pressure examines flame lifting and suppression of combustion oscillation. Flame lifting was evaluated in terms of effects of flame lift-off length and a convex perforated plate configuration was suggested as an effective method for suppressing combustion oscillation.

Figure 13 shows a schematic diagram of the atmospheric pressure single-burner combustion test facility. The main components of the facility were a combustor, air and fuel supply systems, and measuring equipment. The combustor had a cylindrical combustion chamber inside. The air supply system supplied combustion air and cooling air separately to the combustor

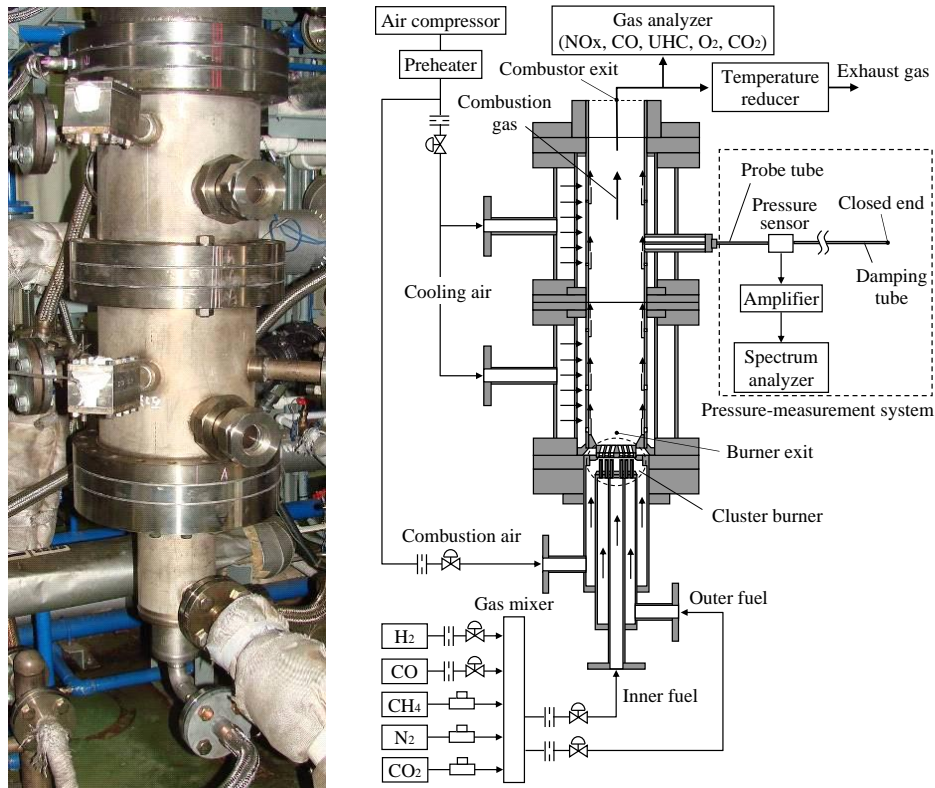


Figure 13. Atmospheric Pressure Single-Burner Combustion Test Facility (Courtesy Asai, et al., 2010, ASME)



from an air compressor through a preheater. The fuel supply system supplied the constituents of the fuel (hydrogen (H₂), carbon monoxide (CO), methane (CH₄), nitrogen (N₂), and carbon dioxide (CO₂)) independently to a gas mixer. The gas mixer produced a gas mixture with certain gas compositions. The compositions of the gas mixture were varied by changing the flowrates of the constituents independently. The gas mixture was separated into the inner fuel and the outer fuel. The measuring equipment consisted of a gas analyzer and a pressure-measurement system.

Figure 14 shows the perforated plate configurations of four types of test burners. The perforated plates, Plate A, Plate B, and Plate C, differed in terms of flame lift-off length and comparison between them could clarify the effects of the flame lift-off length on the burner combustion characteristics. The flame lift-off length was defined as the distance from the plate surface to the flame anchoring point. The flame lift-off length was varied by changing the inclination angle of the central axis of the air holes. Plate D had a convex surface in order to suppress the occurrence of combustion oscillation, whereas Plates A, B, and C had a flat surface. A comparison between Plates B and D with the same flame lift-off length could reveal the effects of plate surface shape on the combustion characteristics.

Table 2 lists the compositions of the four test fuels used in the test. The test fuels were comprised of three constituents: H₂, CH₄, and N₂. The test fuels had approximately equivalent lower heating values per unit volume to the hydrogen content syngas fuels at carbon capture rates of zero, 30, 50, and 90 percent for oxygen-blown IGCC with CCS. Hereafter, the test fuels are referred to as “CCS-0% fuel,” “CCS-30% fuel,” “CCS-50% fuel,” and “CCS-90% fuel.”

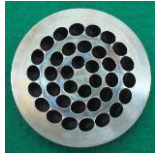



| Perforated plate | Plate A | Plate B | Plate C | Plate D |
|-----------------------|--|--|---|--|
| Surface shape | Flat | Flat | Flat | Convex |
| Photo |  (Front view) |  (Front view) |  (Front view) |  (Front view) (Side view) |
| Flame lift-off length | 0.197 inch (5 mm) | 0.394 inch (10 mm) | 0.591 inch (15 mm) | 0.394 inch (10 mm) |

Figure 14. Perforated Plate Configurations of Test Burners (Courtesy Asai, et al., 2010, ASME)

Table 2. Properties of Test Fuels (Courtesy Asai, et al., 2010, ASME)

| Test fuels | | CCS-0% fuel | CCS-30% fuel | CCS-50% fuel | CCS-90% fuel |
|---------------------|--------------------------------|-------------|--------------|--------------|--------------|
| Constituents: | | | | | |
| H ₂ | vol% | 40.0 | 55.0 | 65.0 | 84.0 |
| CH ₄ | vol% | 18.0 | 15.7 | 6.3 | 2.0 |
| N ₂ | vol% | 42.0 | 29.3 | 28.7 | 14.0 |
| Density | lb/scf [*] | 37.9 | 29.0 | 25.4 | 14.6 |
| | kg/m ³ [*] | 0.641 | 0.490 | 0.429 | 0.246 |
| Lower heating value | Btu/scf [*] | 269.5 | 289.2 | 231.5 | 243.9 |
| | MJ/m ³ [*] | 10.0 | 10.8 | 8.6 | 9.1 |
| | Btu/lb | 6740 | 9446 | 8638 | 15884 |
| | MJ/kg | 15.7 | 22.0 | 20.1 | 36.9 |

^{*} at 70°F, 14.696 psia (294.15 K, 0.10135 MPa)

Flame Lifting

Figure 15 shows NO_x emissions and combustion efficiency for CCS-50% fuel with hydrogen content of 65 volume percent and for Plates A, B, and C at an outer-fuel ratio of 45 percent as a function of burner exit gas temperature. The NO_x emissions decreased with increasing flame lift-off length within the test range. This decrease in NO_x with increasing flame lift-off length is probably due to the increase in the fuel-air mixing length from the burner to the flame front. The increase in



the mixing length enhanced mixing and thus decreased NO_x emissions. The combustion efficiency for each plate decreased with decreasing burner exit gas temperature. The combustion efficiencies for Plates A and B were almost the same, and that for Plate C was the lowest at a burner exit gas temperature of 2375°F (1575 K). This result shows that the increase in the flame lift-off length decreased the flame holding stability. The test finding shows that the increase in the flame lift-off length decreased NO_x emissions but also undesirably decreased flame holding stability.

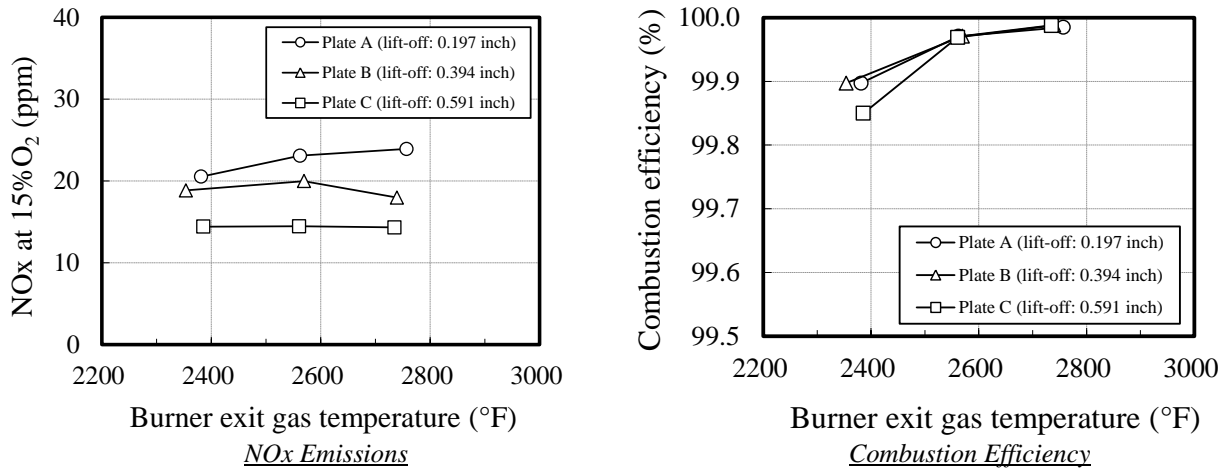


Figure 15. Effects of Flame Lift-off Length (CCS-50% fuel, H₂=65 vol%) (Courtesy Asai, et al., 2010, ASME)

Combustion Oscillation

The cluster burner can minimize NO_x emissions by achieving homogeneous lean combustion. Homogeneous lean combustion can be achieved by supplying fuel to each fuel nozzle at an equal flowrate. This fuel supply yields an outer-fuel ratio of 83.3 percent, which equals the proportion of the number of fuel nozzles in the outer region (30 nozzles) to the total number of fuel nozzles (36 nozzles). Hereafter, this outer-fuel ratio is called a “target ratio.”

Figure 16 shows the variation in NO_x emissions as a function of the outer-fuel ratio for Plate B and CCS-0% fuel at a burner exit gas temperature of 2735°F (1775 K). NO_x decreased when the outer-fuel ratio increased and NO_x yielded the minimum value around the target ratio. However, minimization of NO_x operation may be restricted by the occurrence of combustion

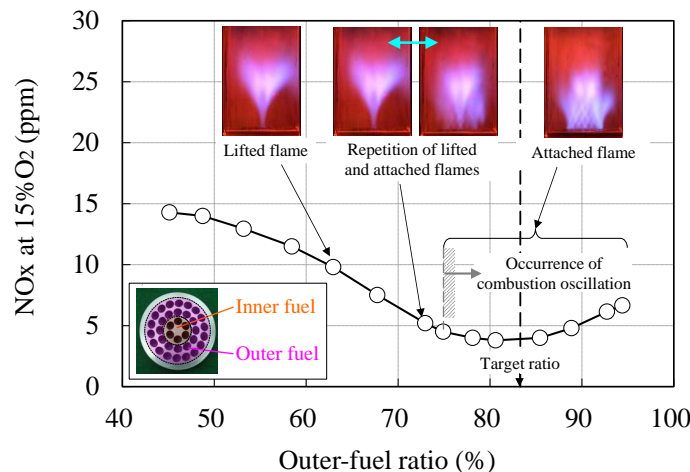


Figure 16. Combustion Oscillation in Cluster Burner for Plate B and CCS-0% fuel (Courtesy Asai, et al., 2011, ASME)



oscillation before the outer-fuel ratio reaches the target ratio. At outer-fuel ratios below around 70 percent, stable lifted flames were formed. At outer-fuel ratios around 72 percent, lifted flame and attached flame repeated alternately. At outer-fuel ratios above 75 percent, the flame attached completely to the perforated plate, and the attached flame fluctuated infinitesimally, thus causing combustion oscillation.

The combustion oscillation may be triggered by the attachment of the flame to the perforated plate due to the ignition of flammable mixtures in the wake behind the plate (Asai, et al. 2010). If amplitudes of pressure fluctuations due to combustion oscillation exceed the criterion, the NO_x minimization may be prevented because the outer-fuel ratio fails to increase up to the target ratio. The NO_x minimization for the cluster burner requires homogeneous lean combustion due to the increase in the outer-fuel ratio up to the target ratio without the occurrence of combustion oscillation.

Suppression of Combustion Oscillation

A cluster burner with a convex perforated plate was suggested as a method to suppress the combustion oscillation (Asai, et al. 2011). Figure 17 shows the concept of the convex perforated plate. The center of the perforated plate projects into the combustion chamber and the surface is inclined. Hereafter, this burner is called the “convex burner.”

The convex burner may be effective in suppressing the combustion oscillation because of the following three effects. First, the convex burner can suppress the ignition of flammable mixtures in the wake behind the plate by positioning the flame away from the plate. The flammable mixtures may be ignited by the combustion gas from the flame as a heat source. When the distance from the plate surface to the flame increases compared with the flat perforated plate, the combustion gas from the flame provides the flammable mixtures with less heat. As a result, the convex burner can suppress the ignition of flammable mixtures. Moreover, the convex burner may be effective in decreasing NO_x emissions because of the increased mixing length. Second, the convex burner can suppress the ignition of flammable mixtures by decreasing the wake size behind the plate. The wake formed behind the convex plate becomes smaller than that behind the flat plate because the growing wake vortices, which are normal to the inclined surface, are swept away by the mixture jet flow. As a result, the convex burner can suppress the ignition of flammable mixtures. Third, the convex burner can suppress the attachment of the flame to the plate by generating the flow along the plate surface. Because the smaller wake vortices allow an outstanding pressure gradient from the outer region to the center of the burner, this pressure gradient enhances the entrainment from the outer region to the center region, thus generating the flow along the plate surface. The flow can blow the approaching flame off the plate surface. As a result, the convex burner can suppress the attachment of the flame to the plate.

Figure 18 compares pressure fluctuation amplitudes and NO_x emissions between Plates B and D for CCS-0% fuel with the hydrogen content of 40 volume percent as a function of the outer-fuel ratio. The burners were tested at a burner exit gas temperature of 2735°F (1775 K). Here, this study defines a certain value of the maximum design amplitude of pressure fluctuations for safely operating the burners. The burners are required to be developed so that they can maintain the pressure fluctuation amplitudes below the maximum design value. The maximum design value is referred to as the criterion of

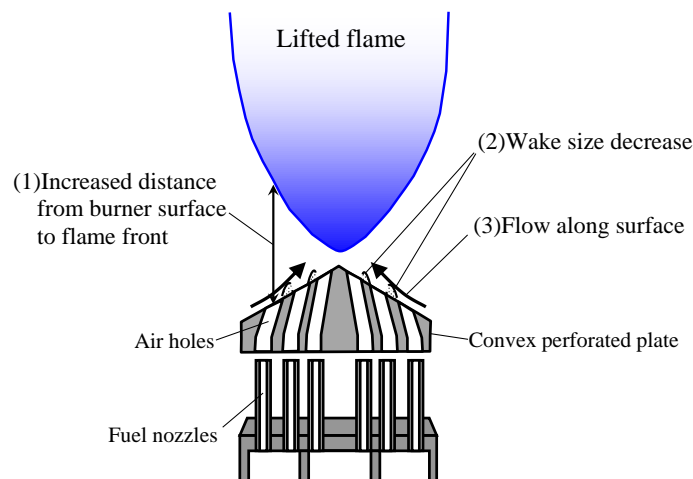
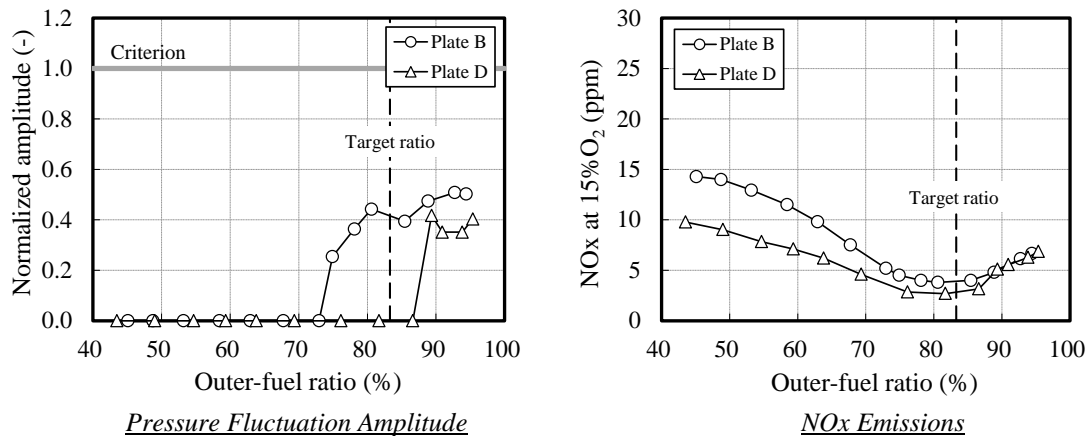


Figure 17. Concept of Convex Burner (Courtesy Asai, et al., 2011, ASME)



combustion oscillation here. The combustion oscillation with an amplitude above the criterion may increase the risk of damage to the burners. In this figure, the amplitude of pressure fluctuation was normalized by the criterion. The combustion oscillation occurred at outer-fuel ratios above 73.0 percent for Plate B and above 86.6 percent for Plate D. The amplitude for Plate D was lower than that for Plate B. The amplitudes for both plates were below the criterion for CCS-0% fuel. This finding shows that Plate D was effective in suppressing the combustion oscillation because Plate D delayed the occurrence of combustion oscillation compared with Plate B. The NO_x emissions for both plates decreased when the outer-fuel ratio increased to below the target ratio (83.3 percent), and yielded the minimum values around the target ratio, and then increased when the outer-fuel ratio increased above the target ratio. This result showed that homogeneous lean combustion was achieved around the target ratio. The higher NO_x emissions at outer-fuel ratios below and above the target ratio were a result of the formation of flames with a higher local equivalence ratio in the inner region and outer region, respectively. Here, the local equivalence ratio was calculated from fuel flowrates supplied to fuel nozzles and air flowrates supplied to air holes in each region. The flames with a higher equivalence ratio formed more NO_x because of their higher flame temperatures. The NO_x emissions for Plate D were lower than those for Plate B within the test range. The difference in NO_x emissions between Plates B and D may be due to the increase in mixing length. The increase in the distance enhanced the fuel-air mixing and thus decreased NO_x emissions.

Figure 19 compares pressure fluctuation amplitudes and NO_x emissions between Plates B and D for CCS-90% fuel with the hydrogen content of 84 volume percent as a function of the outer-fuel ratio. The flame for CCS-90% fuel tended to approach the plate closer because of the higher flame speed. The combustion oscillation emerged at the outer-fuel ratio of 52.6 percent for both plates. However, the amplitude for Plate B exceeded the criterion at outer-fuel ratios above 56.2 percent, and thus the



*Figure 18. Effects of Perforated Plate Surface Shape (CCS-0% fuel, H₂=40 vol%)
 (Courtesy Asai, et al., 2011, ASME)*

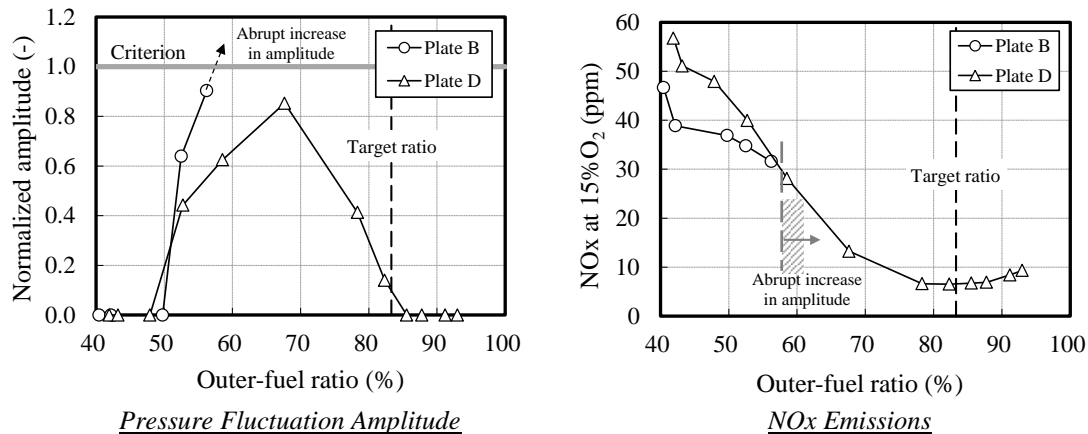


*Figure 19. Effects of Perforated Plate Surface Shape (CCS-90% fuel, H₂=84 vol%)
 (Courtesy Asai, et al., 2011, ASME)*



outer-fuel ratio failed to increase above this ratio. In contrast, the amplitude for Plate D was below the criterion and thus could increase to the target ratio. This finding shows that Plate D was also effective in suppressing the combustion oscillation for CCS-90% fuel. The combustion oscillation emerged at lower outer-fuel ratios for CCS-90% fuel than for CCS-0% fuel. This is most likely due to the higher flame speed for CCS-90% fuel. The flame approached closer, and thus the combustion oscillation tended to occur. The minimum NO_x for Plate B was 31.6 ppm at the outer-fuel ratio of 56.2 percent because the amplitude of pressure fluctuation exceeded the criterion at outer-fuel ratios above this ratio. In contrast, the minimum NO_x for Plate D was 6.5 ppm at the target outer-fuel ratio of 83.3 percent. Thus, Plate D decreased NO_x emissions by increasing the outer-fuel ratio to the target ratio.

Step 2: Combustor Development

In Step 2 (combustor development), single-can combustor configurations are optimized by single-can combustion test at medium to high pressures. Step 1 evaluated performance of the flat burner and the convex burner in order to optimize the burner configuration. This section describes the development of multi-cluster combustors equipped with the flat burner or the convex burner.

Single-Can Combustion Test

Figure 20 shows a schematic diagram of the single-can combustion test facility. A single-can combustor was assembled into the test stand. An air compressor supplied combustion air to the combustor through a preheater, and the pressure in the combustion chamber was adjusted with a back pressure valve downstream. The test fuels consisted of three constituents: H₂, CH₄, and N₂. The fuel supply system independently supplied the following gases to a gas mixer: H₂ from H₂-cylinder-loaded trailers; CH₄ from CH₄-cylinder-loaded trailers; and N₂ from a liquefied nitrogen tank. The gas mixer produced a gas mixture with certain gas compositions as a test fuel. The compositions of the gas mixture were varied by changing the flowrates of the constituents independently. The gas mixture was separated into some fuel circuits. The measuring equipment consisted of a gas analyzer and a pressure-fluctuation-measurement system. The gas analyzer measured gas concentrations in exhaust gas at a measuring duct downstream in the test stand. The pressure-fluctuation-measurement system measured pressure fluctuations inside the combustion chamber.

Figure 21 shows the configurations of two types of test combustors: a flat multi-cluster combustor and a convex multi-cluster combustor (Dodo, et al. 2013). The two combustors differed in terms of the main burner configurations. The flat combustor was equipped with one concave pilot burner at the center and six flat main burners surrounding the pilot burner. The convex combustor was equipped with one concave pilot burner at the center and six convex main burners surrounding the pilot burner. The combustors were tested at a medium pressure under the base load condition.

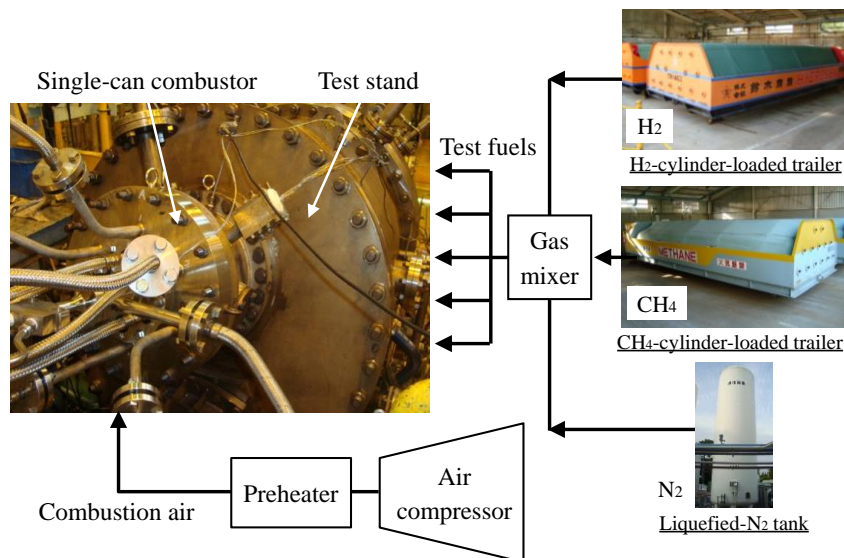


Figure 20. Single-Can Combustion Test Facility



Figure 22 shows variations in pressure fluctuation amplitude and NO_x emissions for the flat combustor as a function of the outer-fuel ratio. Here, the outer-fuel ratio was defined for the main burners. The target outer-fuel ratio was 80 percent, which equaled the proportion of the number of fuel nozzles in the outer region (24 nozzles) to the total number of fuel nozzles (30 nozzles) in each main burner. The amplitude of pressure fluctuation was normalized by the maximum design amplitude for the criterion for safely operating the combustors. For CCS-0% fuel, the flat multi-cluster combustor could increase the outer-fuel ratio up to the target ratio with the amplitude below the criterion, and thus achieved the minimum NO_x at the target ratio. For CCS-30% and CCS-50% fuels, the flat combustor could not increase the outer-fuel ratio to the target ratio because the amplitudes increased abruptly above the criterion before the outer-fuel ratio reached the target ratio. Consequently, the NO_x minimization was restricted by the increase in pressure fluctuation amplitude. In contrast, as shown in Figure 23, the convex multi-cluster combustor could increase the outer-fuel ratio to the target ratio with the amplitude below the criterion for CCS-0%, CCS-30%, and CCS-50% fuels, and thus achieved the minimum NO_x at the target ratio for all the test fuels. Both multi-cluster combustors experienced no flashback throughout the test. The test results show that the convex burner was also effective in suppressing the occurrence of combustion oscillation for full-size combustors.

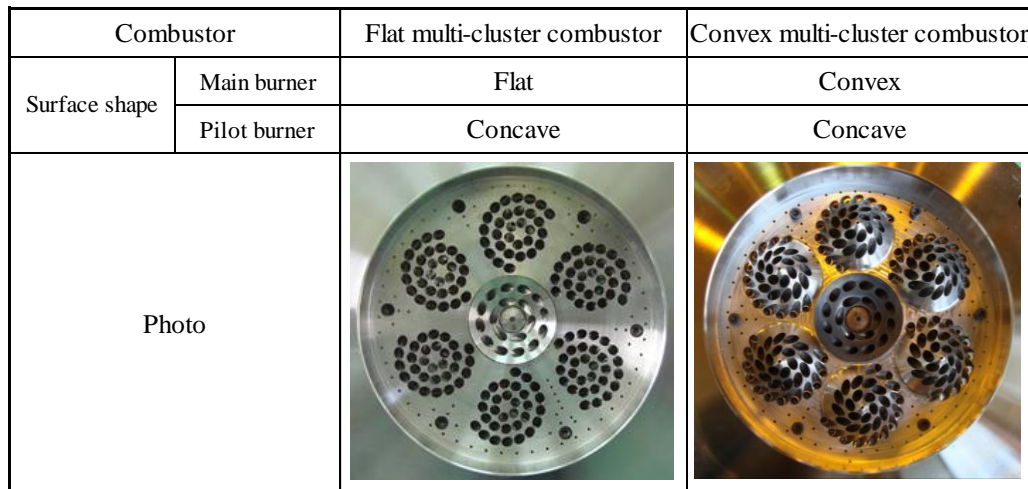


Figure 21. Configurations of Test Combustors (Courtesy Dodo, et al., 2013, ASME)

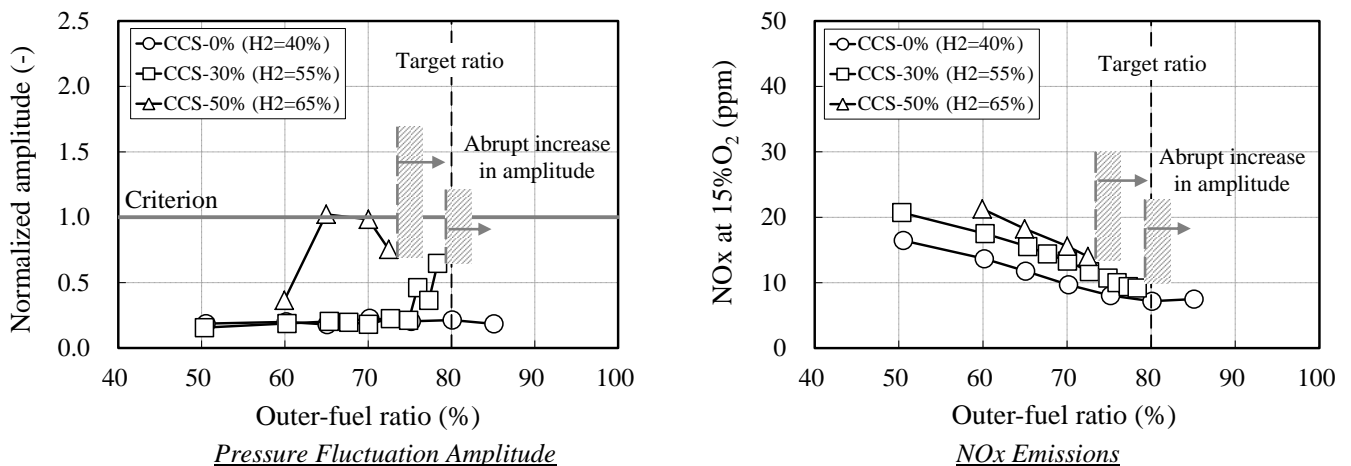


Figure 22. Single-Can Test Results for Flat Multi-Cluster Combustor (Courtesy Dodo, et al., 2013, ASME)

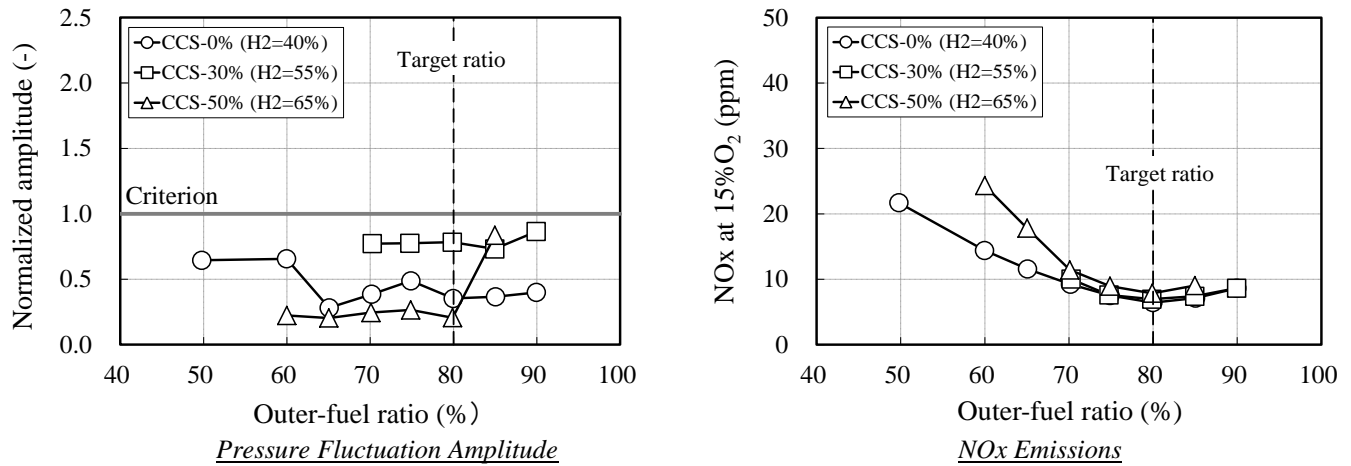


Figure 23. Single-Can Test Results for Convex Multi-Cluster Combustor (Courtesy Dodo, et al., 2013, ASME)

Step 3: Feasibility Demonstration for Practical Plants

Demonstrating the feasibility for IGCC plants requires an evaluation of combustor performance by a real gas turbine test in a multi-can combustor configuration with practical syngas fuel in practical IGCC plants. In order to demonstrate the feasibility for IGCC plants, the combustor was tested with a practical syngas fuel in a multi-can combustor configuration in an IGCC pilot plant (Asai, et al. 2013, 2015a, 2015b).

Field Test Facility

The field test for Step 3 was performed at an oxygen-blown integrated coal gasification power generation pilot plant named EAGLE (an acronym for “coal Energy Application for Gas, Liquid and Electricity”) (Kimura 2005, Nagasaki, et al. 2010, Nagasaki, et al. 2013, Omata 2014) located at the Wakamatsu Research Institute of the Electric Power Development Co., Ltd., Japan (J-POWER). The EAGLE plant (Figure 24) was a test facility for developing coal gasification technologies with innovative CO₂ capture. The EAGLE plant consisted of five main components: an air separation unit (ASU); a gasifier; a gas cleanup unit; a gas turbine; and a CO₂ capture unit. The ASU separated air into nitrogen and oxygen. The nitrogen was supplied to the gas turbine as a diluent in order to suppress the NO_x emissions during oil-fuel operation. The oxygen was supplied to the gasifier as an oxidant for the gasification process. The gasifier converted coal to raw syngas by reacting it with oxygen. The gasifier employed an oxygen-blown, single-chamber, two-stage, swirling-flow entrained bed gasification method. The gas cleanup unit removed impurities from the raw syngas, producing a clean syngas. The clean syngas was supplied separately to the gas turbine and the CO₂ capture unit. This separate syngas supply was due to the field test operational circumstance that the test of the gas turbine combustor proceeded simultaneously with the test of the CO₂ capture individually in the test series.

The flat multi-cluster combustor was employed for the test because it was applicable to such a medium hydrogen content fuel and its structural reliability was ensured by the simple structure of the flat perforated plate. This multi-cluster combustor for the IGCC was developed for F-class gas turbines. The fuel supply systems supply syngas fuel and oil fuel to the combustor. Figure 25 shows the fuel supply systems for the combustor. The main burners are divided into two groups (F2 and F3) consisting of three burners each, and they are arranged alternately surrounding the pilot burner (F1) at the center. The syngas fuel is distributed into five fuel circuits: F1 fuel to the F1 pilot burner; F2-1 fuel to the inner region; F2-2 fuel to the outer region of the F2 main burners; F3-1 fuel to the inner region; and F3-2 fuel to the outer region of the F3 main burners. The oil fuel is supplied to the oil spray nozzle. The combustor can achieve low emissions and high operability over the entire operating range by switching combustion modes according to operating conditions. The combustor switches the modes by manipulating the combination of operating burners for which the fuel circuit is fueled.

The syngas fuel burned for the tests was comprised mainly of CO, H₂, and N₂. The syngas fuel contained approximately 50 percent CO, 20 percent H₂, and 20 percent N₂ by volume. Distillate oil was also burned for oil fuel operation between ignition and



a part load. The EAGLE pilot plant test was conducted from startup on distillate oil to the maximum load (corresponding to 80 percent of the gas turbine load) on syngas produced in the test series.

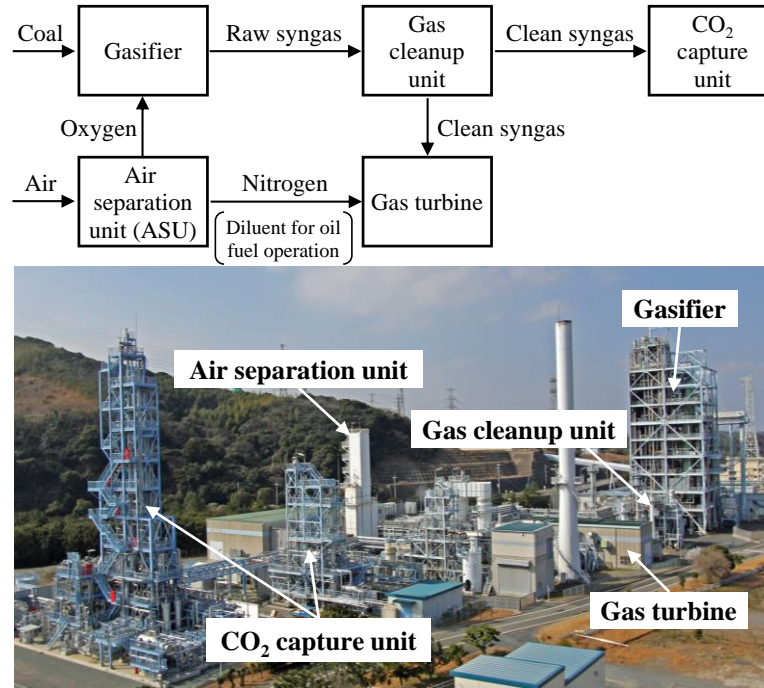


Figure 24. EAGLE Pilot Plant (Photo Courtesy of J-POWER)

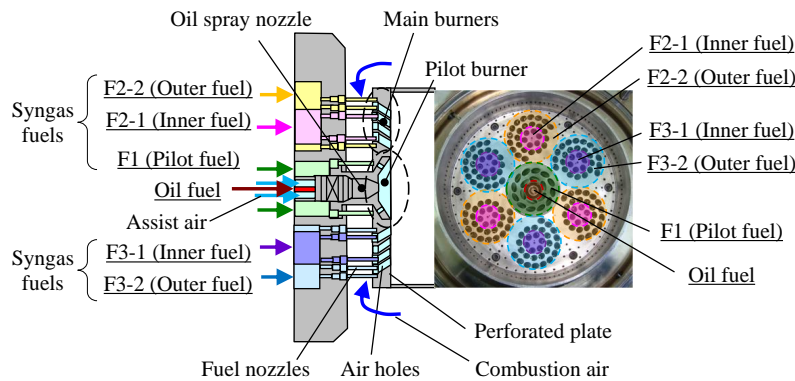


Figure 25. Fuel Supply Systems (Courtesy Asai, et al., 2015b, ASME)

Combustor Performance at Maximum Load

This section evaluates the performance of the combustor at a maximum gas turbine load of 80 percent. The combustor operated all the syngas-fueled burners at the maximum gas turbine load. Figure 26 shows the NO_x emissions at the maximum load as a function of the outer-fuel ratio defined for the main burners. The NO_x emissions decreased with increasing outer-fuel ratio until reaching the target ratio (80 percent), yielded the minimum value at the target ratio, and then increased again with increasing outer-fuel ratio above the target ratio. The NO_x emissions yielded the minimum value of 10.9 ppm at the target ratio.

Figure 27 compares NO_x emissions between the multi-cluster combustor and the diffusion-flame combustor at the maximum load as a function of the normalized mass flowrate ratio of injected diluent nitrogen to syngas fuel. The data for the multi-cluster combustor yielded the minimum NO_x of 10.9 ppm. The data for the diffusion-flame combustor were acquired in the test of the



combustor in the same pilot plant. The multi-cluster combustor achieved low NO_x around 10 ppm at a N₂/fuel ratio of zero (i.e., diluent-free (dry)). In contrast, the diffusion-flame combustor yielded much higher NO_x around 200 ppm at a N₂/fuel ratio of zero, and required diluent nitrogen to cut NO_x to the same level at which the multi-cluster combustor achieved a diluent-free condition. This comparison demonstrated that the multi-cluster combustor achieved the dry low-NO_x combustion of the syngas fuel in the IGCC pilot plant.

Figure 28 shows combustion efficiency plotted against the outer-fuel ratio. The combustion efficiency attained high values of over 99.95 percent at the target ratio. This result demonstrated that the multi-cluster combustor achieved complete combustion of the syngas fuel at the maximum load in the IGCC pilot plant.

Regarding stability, Figure 29 shows the maximum amplitudes of pressure fluctuations in all the cans at the maximum load versus the outer-fuel ratio. The pressure fluctuation amplitude was normalized by the maximum design amplitude for the criterion for safely operating the combustor. The multi-cluster combustor maintained the amplitude at low values well below the criterion over the entire test range. This result demonstrated that the combustor achieved stable operation with low levels of pressure fluctuations.

Regarding reliability, Figure 30 shows the maximum values of all combustion liner and perforated plate metal temperatures in all the cans versus the outer-fuel ratio. Here, this study defines a certain value of the maximum design metal temperature for safely operating the combustor. The combustor is required to be developed so that they can maintain the metal temperatures below the maximum design value. This study judges that reliability is ensured when the combustor maintains the metal temperatures below the maximum design value. The maximum design value is referred to as the criterion of metal temperatures here. The ordinate in this figure denotes the relative value of the maximum metal temperature in all the cans normalized by the maximum design value. The multi-cluster combustor maintained the liner and perforated plate metal temperatures at values below the criterion over the

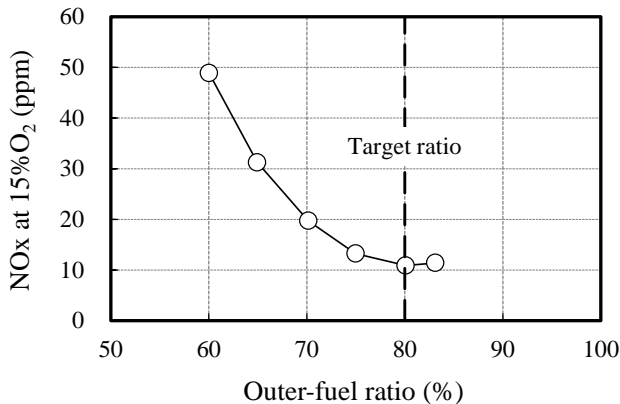


Figure 26. NO_x Emissions at Maximum Load (Courtesy Asai, et al., 2015a, ASME)

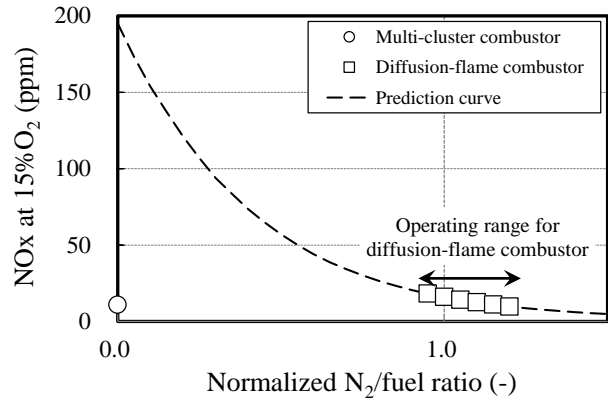


Figure 27. Comparison of NO_x between Multi-Cluster and Diffusion-Flame Combustors (Courtesy Asai, et al., 2015a, ASME)

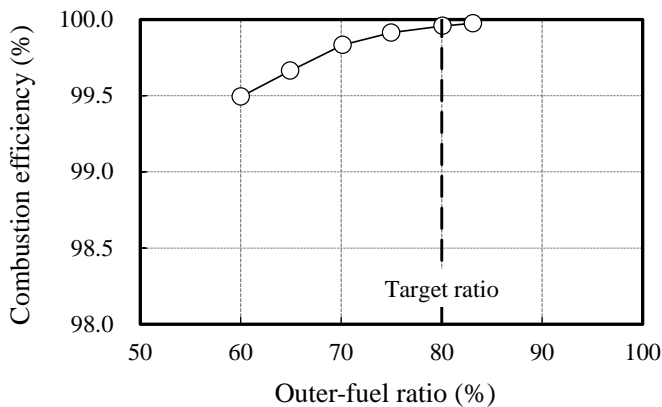


Figure 28. Combustion Efficiency at Maximum Load (Courtesy Asai, et al., 2015a, ASME)

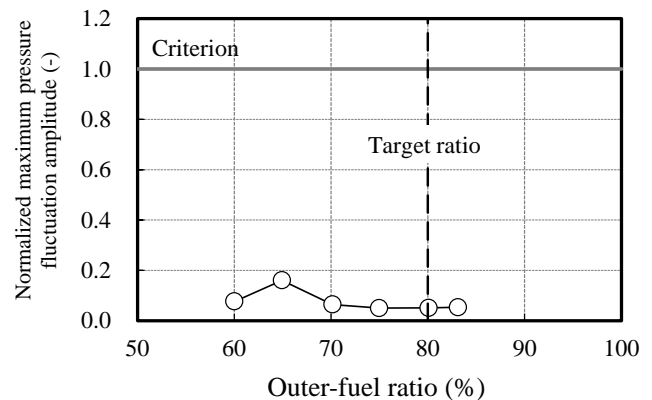


Figure 29. Pressure Fluctuation Amplitude at Maximum Load (Courtesy Asai, et al., 2015a, ASME)



entire test range. These test results demonstrated that the multi-cluster combustor achieved reliable operation with low metal temperatures of the liners and plates below the criterion. The multi-cluster combustor experienced no flashback throughout the test. In summary, these test results demonstrated the feasibility of achieving the DLN and flashback-resistant combustion by the multi-cluster combustor for practical IGCC plants.

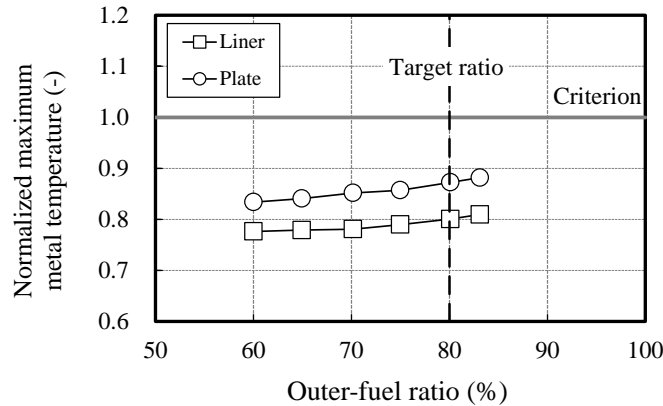


Figure 30. Metal Temperatures at Maximum Load (Courtesy Asai, et al., 2015a, ASME)

Combustor Performance at Part Load

The combustor is required to operate stably from ignition through part load to the base load in practical IGCC plants. This section describes evaluation of the performance of the combustor at part load.

The combustor can achieve low emissions and high operability over the entire operating range by switching combustion modes according to operating conditions. Figure 31 shows the two fuel staging sequences (“staging I” and “staging II”) and combustion modes (Asai, et al. 2015b). In this figure, colored regions shown on the burner pictures indicate operating burners. Staging I is the initial method. Staging I consists of three distinct combustion modes designated as mode O, mode C, and mode A. Staging I switches

| Operating range | | Turbine speed (%) | Low ← | Gas turbine load (%) | → High |
|--------------------------|-------------------|-------------------|-------|-------------------------|--------------------------------|
| Fuel | | Oil | | Syngas | |
| Staging I (Initial) | Mode | Mode O | | Mode C | Mode A |
| | Operating burners | Oil spray nozzle | | F1 + F2-1 + F3-1 | F1 + F2-1 + F2-2 + F3-1 + F3-2 |
| | | | | | |
| Staging II (Advanced) | Mode | Mode O | | Mode D | Mode A |
| | Operating burners | Oil spray nozzle | | F1 + F2-1 + F2-2 + F3-1 | F1 + F2-1 + F2-2 + F3-1 + F3-2 |
| | | | | | |

Figure 31. Fuel Staging Sequences and Combustion Modes (Courtesy Asai, et al., 2015b, ASME)



from mode O, through mode C, to mode A between ignition and base load. Mode O is employed as an oil mode with the oil spray nozzle for oil fuel operation from ignition to a part load. Mode C is employed as a partial mode with the pilot burner (F1) and inner regions of the main burners (F2-1 and F3-1) for syngas operation at part load. Mode A is employed as the final mode with the pilot burner (F1) and all the main burners (F2-1, F3-1, F2-2, and F3-2) for syngas operation to base load. Switching loads between the combustion modes hinge on operating conditions or environmental regulations. Staging II is an advanced method. Staging II is suggested in order to improve the combustor’s part load performance. Staging II employs mode D with F1, F2-1, F3-1 and F2-2 circuits fueled as an alternative partial mode to mode C in staging I. Mode D is a hybrid of modes C and A. Mode C features localized fuel-rich combustion zones of the inner regions of the main burners (F2-1 and F3-1). The localized zones operate at high flame temperatures due to high equivalence ratios near unity. Mode C thus achieves high combustion efficiency at low loads, whereas mode C causes high NO_x at high loads. Mode A features dispersed fuel-lean combustion zones of the inner and outer regions of the main burners (F2-1, F3-1, F2-2 and F3-2). The dispersed zones operate at relatively low flame temperatures due to low equivalence ratios. Mode A thus causes low combustion efficiency at low loads, whereas mode A achieves low NO_x at high loads. Mode D is an intermediate form between modes C and A to function in staging II in order to improve combustor performance. Mode D can achieve lower NO_x than mode C due to the lower flame temperatures of F2-1 and F2-2. Mode D can achieve higher combustion efficiency than mode A due to the higher flame temperatures of F3-1.

Figure 32 shows the variations in NO_x emissions for staging I and staging II as a function of the gas turbine load. In this figure, the circles and squares indicate the data for staging I and staging II, respectively. For each staging, the solid and open symbols indicate the data for oil fuel operation and syngas operation, respectively. Both stagings periodically increased and decreased NO_x emissions with the load. Both stagings increased NO_x with the load in each combustion mode, and decreased NO_x at each mode-switching load. Staging I yielded maximum NO_x of 75 ppm at 50 percent load in mode C. This behavior implies that NO_x is probably higher in mode C above 50 percent load. The probable increases in NO_x restrict the load-up in mode C above 50 percent load. Staging II yielded a lower NO_x of 34 ppm at 50 percent load and maximum NO_x of 44 ppm at 60 percent load in mode D. The test results demonstrated that staging II comprising mode D improved NO_x performance at part load.

Figure 33 shows combustion efficiency for staging I and staging II, as plotted against the gas turbine load. Both stagings periodically increased and decreased the combustion efficiency with the load. Both increased the combustion efficiency with the load in each mode, and decreased the combustion efficiency at each mode-switching load. Staging I sharply decreased the

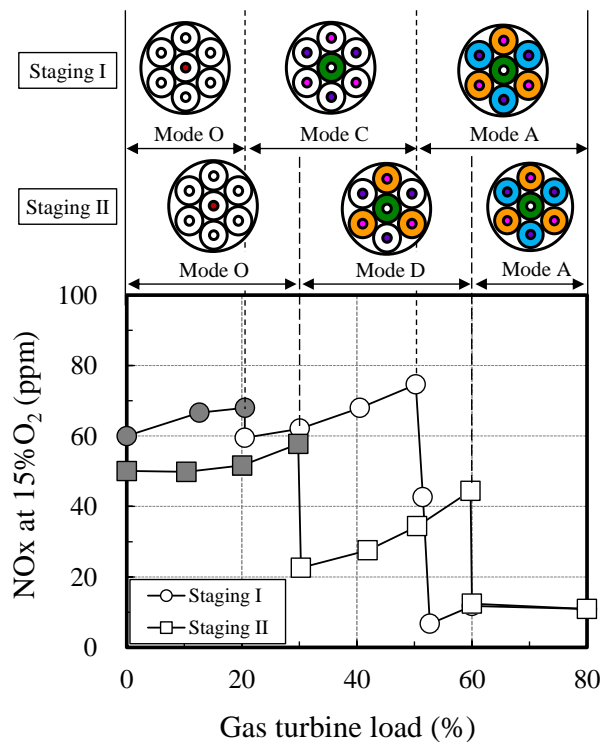


Figure 32. NO_x Emissions at Part Load
 (Courtesy Asai, et al., 2015b, ASME)

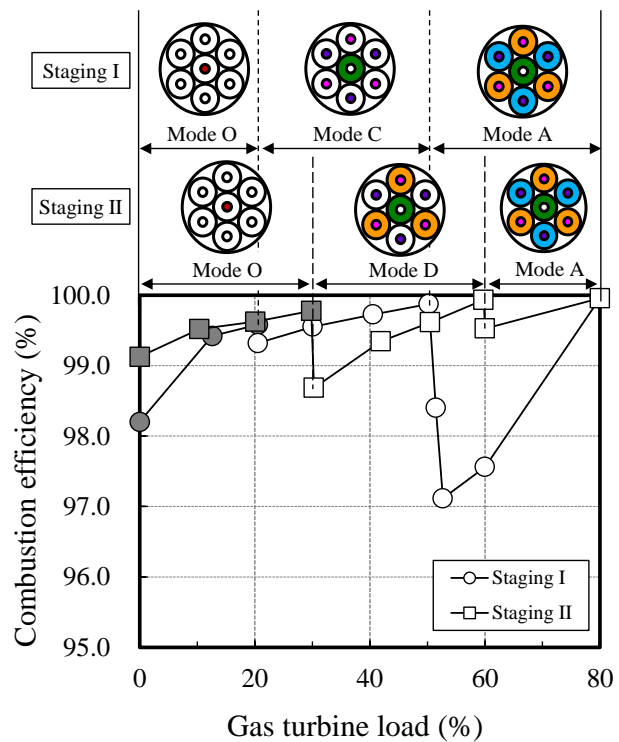


Figure 33. Combustion Efficiency at Part Load
 (Courtesy Asai, et al., 2015b, ASME)



combustion efficiency from 99.9 to 97.1 percent when switching from mode C to mode A at 50 percent load. The sharp decrease in combustion efficiency was the main disadvantage of staging I. This disadvantage yielded insufficient part load performance. Staging II decreased the combustion efficiency from 99.8 to 98.7 percent when switching from mode O to mode D at 30 percent load, and decreased the combustion efficiency from 99.9 to 99.5 percent when switching from mode D to mode A at 60 percent load. The decreases in combustion efficiency at 30 and 60 percent load were smaller than those at 50 percent load for staging I. Staging II attained higher combustion efficiency above 98.7 percent over the part load range, particularly between 50 and 60 percent load. Staging II improved the combustion efficiency performance at part load by operating mode D in the range between 50 and 60 percent load, where staging I yielded insufficient combustion efficiency. The differences in combustion efficiency in mode A at 60 percent load between stagings I and II were probably due to the effect of modes C or D on transient behaviors during operation.

Regarding stability, Figure 34 shows the maximum amplitudes of pressure fluctuations in all the cans for staging I and staging II versus the gas turbine load. Both stagings maintained the amplitudes at low values well below the criterion over the part load range. The results demonstrated that both achieved stable operation at part load with low levels of pressure fluctuations.

Regarding reliability, Figure 35 shows the maximum values of all combustion liner metal temperatures in all the cans for staging I and staging II versus the gas turbine load. Both stagings maintained the liner metal temperatures at low values below the criterion over the part load range. Both increased the liner metal temperatures with the load during oil or syngas operation, and decreased the liner metal temperatures when switching from oil to syngas operation. The test results demonstrated that both stagings achieved reliable operation at part load with low liner metal temperatures below the criterion. Both experienced no flashback throughout part load.

In summary, the test results demonstrated the feasibility of the multi-cluster combustor for achieving dry low-NO_x and flashback-resistant combustion of the H₂ content syngas fuel with high stability, reliability and operability in the IGCC pilot plant. Based on the experience in the field test, a multi-cluster combustor was developed and installed on a 100 MW class gas turbine in an oxygen-blown IGCC demonstration plant of the OSAKI CoolGen Corporation, Japan (Nagasaki and Akiyama 2014, Dodo, et al. 2015). This demonstration plant is part of a project funded by the Japanese Government. Its demonstration test will start in March 2017.

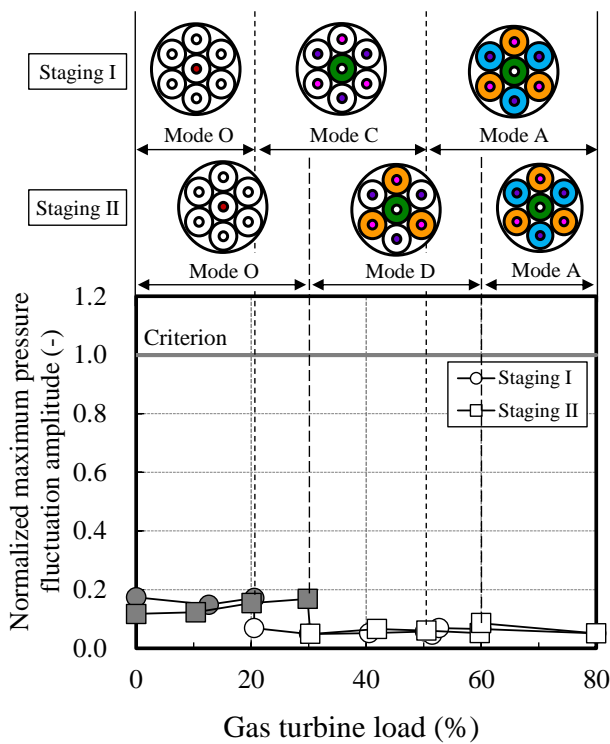


Figure 34. Pressure Fluctuation Amplitude at Part Load
 (Courtesy Asai, et al., 2015b, ASME)

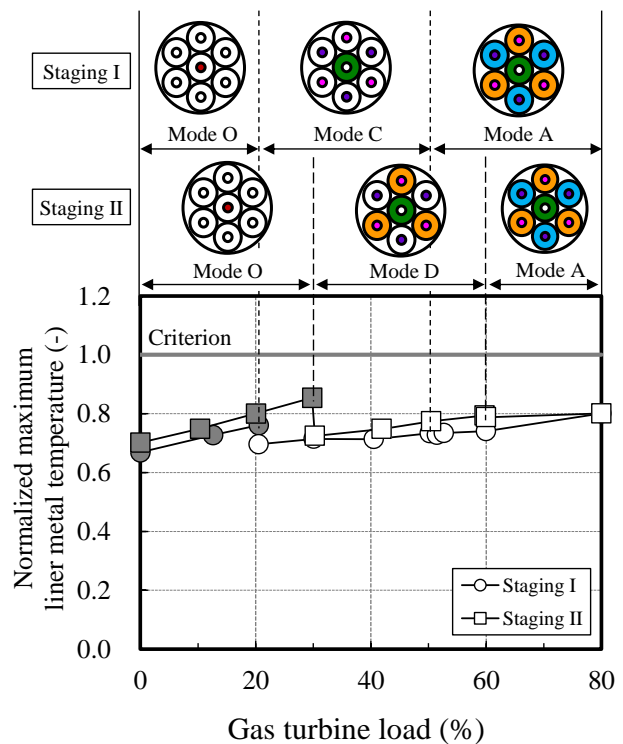


Figure 35. Liner Metal Temperatures at Part Load
 (Courtesy Asai, et al., 2015b, ASME)



Development of Numerical Simulation Technology

Numerical simulation technology will become a powerful tool for developing gas turbine combustors because it provides the details of combustion flows. Numerical simulation technology will contribute to enhancing combustor performance and to cutting development cost and time. Many research groups, gas turbine manufacturers, and simulation software developers have been developing numerical simulation technology extensively targeting applications to development of gas turbine combustors.

Gas turbine combustors, particularly multi-cluster combustors, generate complicated turbulent combustion flows because they may form mixed flows between diffusion-flame combustion and premixed combustion. Hence, numerical simulation tools for multi-cluster combustors are required to analyze diffusion-flame and premixed combustion types seamlessly. This section outlines a numerical simulation tool that has been developed by Yunoki, et al. (2013) in order to analyze both combustion types seamlessly.

Table 3 summarizes the turbulent combustion model that is incorporated in this simulation tool. This model consists of a turbulence model and a combustion model. The turbulence model is a large eddy simulation (LES) with dynamic subgrid scale (SGS) model (Murota 2003). The LES models dissipation effects due to turbulent eddies that are smaller than the computational cell size, and it analyzes turbulent flows that are larger than the computational cell size by solving the basic flow equations. The dynamic SGS models energy transfer due to eddy viscosity. The combustion model is a hybrid turbulent combustion (HTC) model, which is a combination of a flamelet/progress variable (FPV) model and a flame propagation model. The FPV model is generally applied to diffusion flames. It requires a database “flamelet library,” which is obtained by calculation of laminar flame under various conditions. The flame propagation model is applied to premixed flames and it considers the flame stretch effect, the diffusion enhancement effect, and the increasing rate of the flame surface area.

Table 3. Turbulent Combustion Model in the Simulation Tool (Courtesy Yunoki, et al., 2013, ASME)

| Model | |
|------------|---|
| Turbulence | Large Eddy Simulation (LES) with Dynamic SubGrid Scale (SGS) Model |
| Combustion | Hybrid Turbulent Combustion (HTC) Model: Combination of - Flamelet/Progress Variable (FPV) Model for diffusion-flame combustion - Flame Propagation Model for premixed combustion |

This simulation tool was employed to simulate a cluster burner combustion flow for methane at atmospheric pressure in order to validate the turbulent combustion model. Figure 36 shows simulation results for distributions of instantaneous and time-averaged temperatures normalized by the difference from the lowest temperature. The instantaneous distribution on the left-hand side shows that the central region included much higher temperatures than the outer region did because burned gas was backflowed to the burner central region by the recirculation flow. The time-averaged distribution on the right-hand side shows that the central region had a uniform temperature due to combustion of the homogeneous fuel-air mixture.

Figure 37 compares the simulation results with experiments in terms of temperature, and oxygen (O₂) and methane (CH₄) concentrations in the radial direction at an axial distance (z) of 60 mm. The simulation results were time-averaged quantities. The calculated gas temperatures agreed well with experimental data. The simulation predicted the tendency that temperature decreased from the internal to the outer sides in the combustion chamber and temperature was uniform from the center to the radial distance of 20 mm. The calculated O₂ and CH₄ concentrations also agreed well with experimental data. The HTC model succeeded in predicting the position of the oxidation reaction in fuel (radial distance: 20 mm). This comparison demonstrates the validity of this turbulent combustion model for atmospheric CH₄-fuelled combustion by the cluster burner.

However, there are not sufficient experimental data available for validation nor are there accurate chemical reaction models available, especially for a wide variety of fuels at high pressures. Validation of the turbulent combustion model for various fuels and high pressures requires increasing experimental data available for such validation and developing accurate chemical reaction models.

Air hole passages of cluster burner

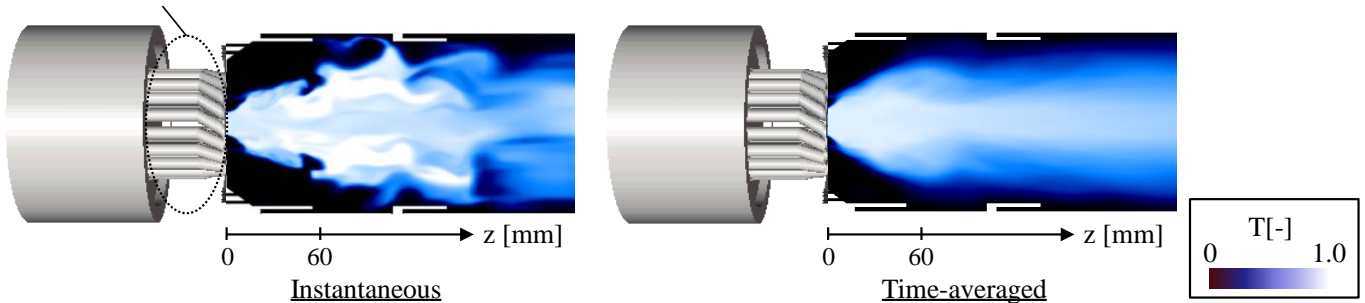


Figure 36. Simulation Results for Temperature of Cluster Burner Combustion Flow for Methane at Atmospheric Pressure (Courtesy Yunoki, et al., 2013, ASME)

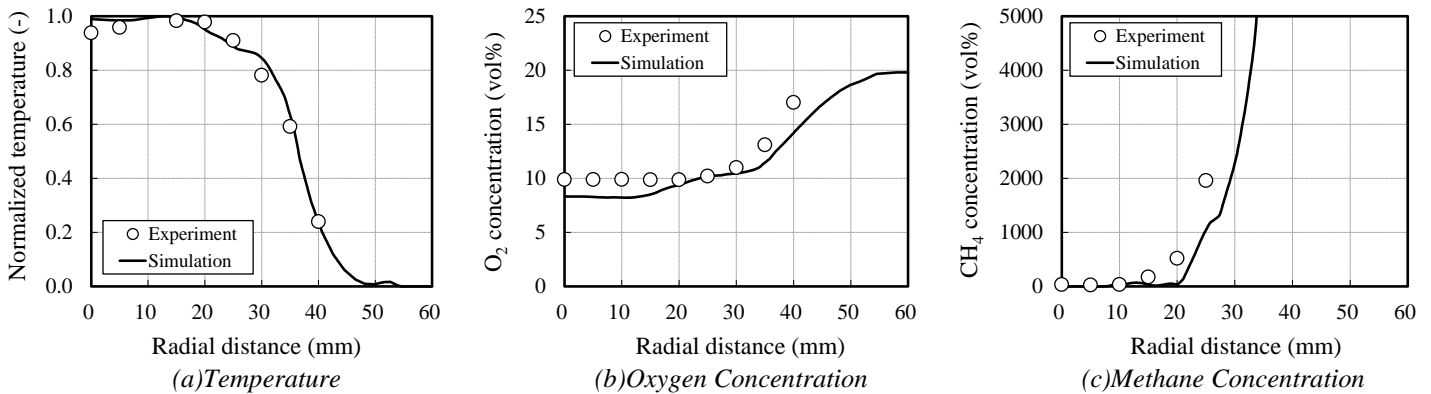


Figure 37. Comparison between Simulation and Experiment (Axial Distance $z=60$ mm) (Courtesy Yunoki, et al., 2013, ASME)

EXPANDING FUEL FLEXIBILITY

The multi-cluster combustor holds great potential for application to a wide variety of fuels and hence, to expand fuel flexibility. This section describes such applications of the multi-cluster combustor.

Dimethyl Ether (DME)

Dimethyl ether (DME), having the chemical formula CH_3OCH_3 , is currently attracting attention as a promising clean alternative fuel; it is clean owing to its low sulfur oxides (SO_x) and low soot emissions. Moreover, it is producible from various hydrocarbon materials. Table 4 compares fuel properties of DME, propane, and methane. DME has a lower autoignition temperature and higher flame speed compared with propane and methane. Its low autoignition temperature of 662°F (623 K) may be lower than the compressor-discharged air temperatures. This property increases the risk of autoignition of DME in a premixing section when it is burned by premixed combustors. In addition, its high flame speed increases the risk of flashback into the premixing section.

The multi-cluster combustor is suitable for combustion of DME with such properties because the short premixing section of the combustor can decrease the risk of autoignition and flashback. Hence, the multi-cluster combustor was developed for DME (Kobayashi, et al. 2003, Saitou, et al. 2004, Saitou, et al. 2005). Figure 38 shows the configuration of the multi-cluster combustor developed for DME. The combustor is equipped with a pilot burner at the center and six main burners surrounding the pilot burner. The combustor was tested with DME at high pressures in the single-can combustion test facility in order to demonstrate the feasibility of achieving dry low- NO_x and flashback-resistant combustion of DME. Figure 39 shows NO_x emissions as a function of the gas turbine load. The combustor operated in four distinct combustion modes by switching the modes according to the gas turbine load. The combustor emitted NO_x of about 70–150 ppm below 50 percent load, however, it achieved low NO_x of less than 24 ppm above



60 percent load by dispersing fuel to all the burners. The combustor experienced no flashback throughout the tests. The test results demonstrated the feasibility of achieving dry low-NO_x and flashback-resistant combustion of DME by the multi-cluster combustor.

This feasibility demonstration for DME implies that the multi-cluster combustor will be applicable to liquefied petroleum gas (LPG) and liquefied natural gas (LNG). LPG and LNG are widely used as gas turbine fuels. LPG contains propane and LNG contains methane as their main component. Propane and methane may pose low risk of autoignition and flashback because of their lower autoignition temperatures and lower flame speeds compared with DME. Hence, the multi-cluster combustor will also be applicable to LPG and LNG.

Table 4. Fuel Properties (Courtesy Saitou, et al., 2005, ASME)

| Properties | Unit | DME | Propane | Methane |
|-----------------------------|---------------------|----------|---------|----------|
| Density | lb/scf* | 113.2 | 107.7 | 39.6 |
| | kg/m ³ * | 1.91 | 1.82 | 0.67 |
| Heating value | Btu/lb | 12425 | 19992 | 21582 |
| | MJ/kg | 28.9 | 46.5 | 50.2 |
| Flammability limit | vol% | 3.4–17.0 | 2.1–9.5 | 5.0–15.0 |
| Adiabatic flame temperature | °F | 3866 | 3852 | 3792 |
| | K | 2403 | 2395 | 2362 |
| Autoignition temperature | °F | 662 | 939 | 1170 |
| | K | 623 | 777 | 905 |
| Laminar flame speed | inch/s | 19.7 | 16.9 | 14.6 |
| | cm/s | 50.0 | 43.0 | 37.0 |

* at 70°F, 14.696 psia (294.15 K, 0.10135 MPa)

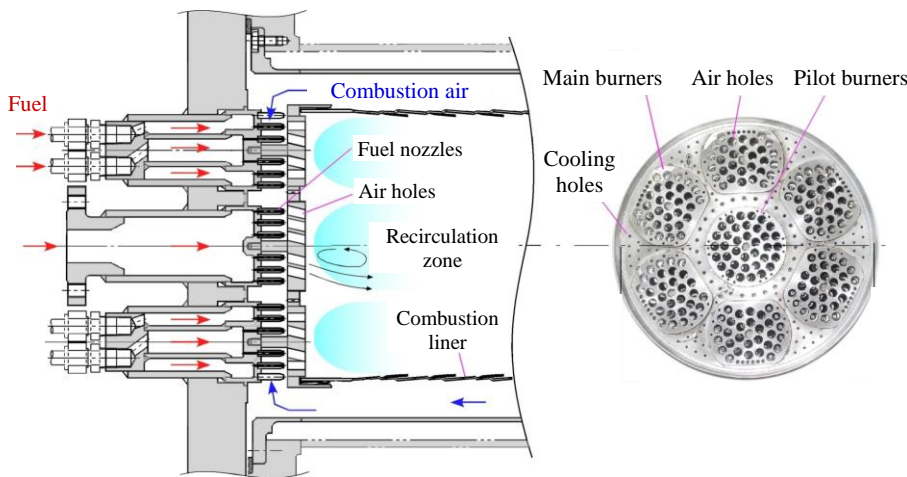


Figure 38. Configuration of Multi-Cluster Combustor for DME (Courtesy Saitou, et al., 2005, ASME)

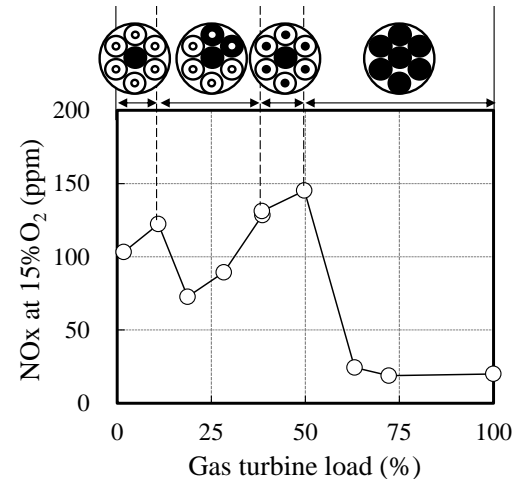


Figure 39. NO_x in Single-Can Combustion Test (Courtesy Saitou, et al., 2005, ASME)

Combustion with Humidified and High-Temperature Air

The multi-cluster combustor is applicable to combustion with humidified and high-temperature air. Humidified air is effective in decreasing NO_x emissions, however diffusion-flame combustors have their limits to decreasing NO_x even at a humidified air condition. High-temperature air increases the risk of flashback and autoignition. Thus, the multi-cluster combustor is suitable for low-NO_x and flashback-resistant combustion with humidified and high-temperature air. This combustion technology with humidified and high-temperature air is applicable to the advanced humid air turbine (AHAT) system (Higuchi, et al. 2008). The AHAT system



uses humid air and a heat recovery system, and it offers the advantage of high thermal efficiency without using an extremely high combustion temperature, pressure ratio, or an intercooler.

Figure 40 shows a schematic diagram of the AHAT system. A water atomization cooling (WAC) unit is installed in the compressor's inlet duct, from which fine water droplets are sprayed. Some water droplets evaporate at the compressor inlet and cool the inlet air. The remaining droplets evaporate while being compressed in the compressor; thus they suppress a rise in air temperature. The compressed air contacts directly with hot water in the humidifier and forms high humidity air. Consequently, the flowrate and specific heat of the working fluid increase, thus increasing turbine generation power. Very moist air flows into the combustor after being preheated by the turbine exhaust gas with the recuperator. The high temperature combustion gas drives the turbine and transfers its exhaust heat to the recuperator and economizer. The exhaust gas that exits the economizer contacts directly with the cold water in the water recovery unit to be cooled and the moisture condenses. The exhaust gas that exited the water recovery unit is then discharged into the atmosphere from a stack after being reheated by the superheater.

Figure 41 shows the configuration of the multi-cluster combustor developed for the AHAT system (Koganezawa, et al. 2007, Abe and Koganezawa 2013). The combustor is equipped with 238 pairs of a fuel nozzle and an air hole that are installed coaxially. The pairs form eight concentric circles. The central four circles are the first section (F1). The fifth circle is the second section (F2) and the sixth and seventh circles are the third section (F3). The last (outermost) circle is the fourth section (F4). A portion of the second section through the fourth section is the fifth section (F5). This multi-cluster combustor was tested in a multi-can configuration on a gas turbine in the 40 MW class AHAT test facility (Figure 42). Figure 43 shows the facility test results for effects of air humidity on NO_x

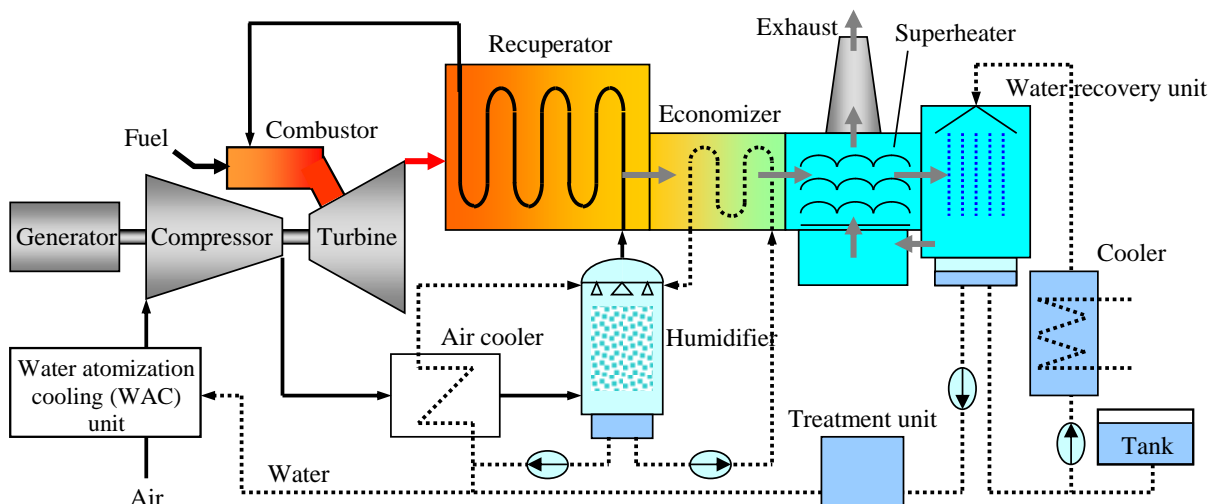


Figure 40. Schematic Diagram of AHAT System (Courtesy Koganezawa, et al., 2007, ASME)

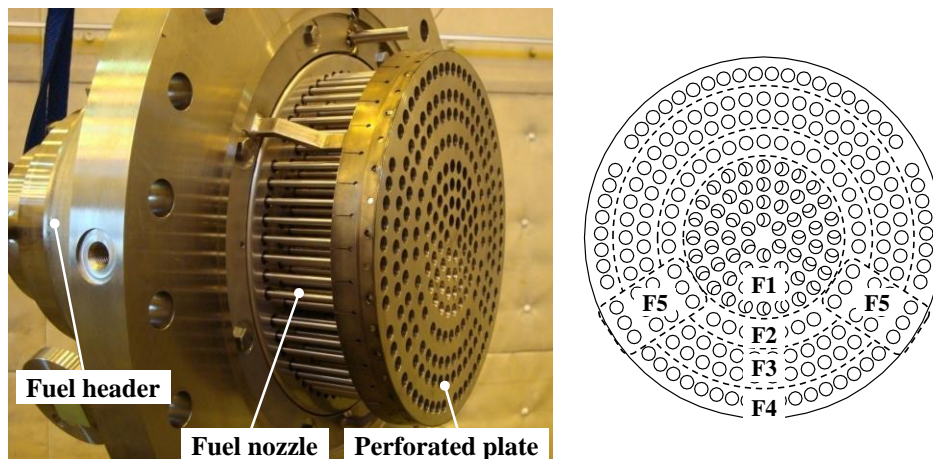


Figure 41. Configuration of Multi-Cluster Combustor for AHAT System (Courtesy Abe and Koganezawa, 2013, CSPE)



emissions, including the single-can test results. The logarithms of NO_x emissions are proportional to air humidity. In the test facility, the humidity was limited to values below 11 volume percent due to the capability of the humidifier. In the facility test, the NO_x emissions were 24 ppm at an air humidity of 11 volume percent. In the single-can test, the NO_x emissions achieved single digit values at an air humidity of 16.3 volume percent. The data for both the facility test and the single-can test lay on the same line. Hence, the multi-cluster combustor will achieve NO_x of less than 10 ppm if the humidifier can supply the combustion air with air humidities of over 16 volume percent in a future commercial AHAT plant.

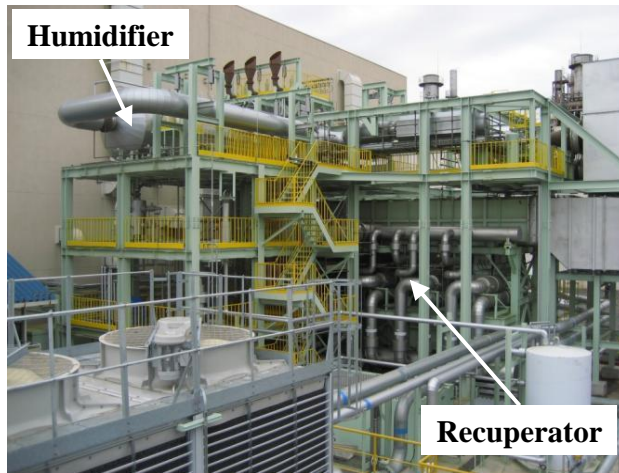


Figure 42. 40 MW Class AHAT Test Facility
 (Courtesy Abe and Koganezawa, 2013, CSPE)

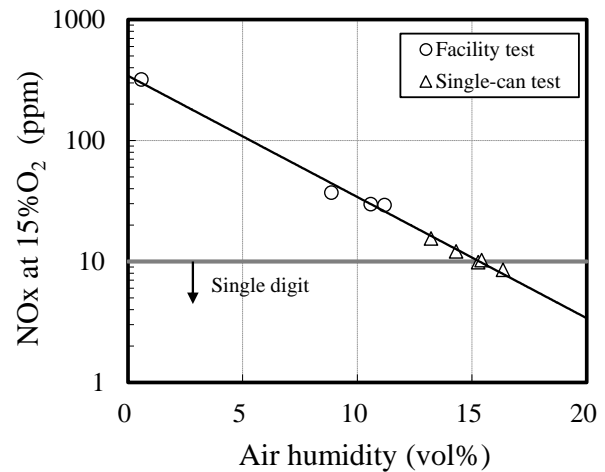


Figure 43. Test Results for Effects of Air Humidity on NO_x
 (Courtesy Abe and Koganezawa, 2013, CSPE)

CONCLUSIONS

This paper described the development of the multi-cluster combustor as an advanced dry low-NO_x and flashback-resistant combustion technology for fuel flexible gas turbines. The combustor consists of multiple fuel nozzles and multiple air holes. The essence of the burner concept is the integration of two key technologies: low-NO_x combustion due to the enhancement of fuel-air mixing; and flashback-resistant combustion due to short premixing sections, air-stream-surrounded fuel jets and lifted flames.

The combustor has been developed particularly for hydrogen content syngas fuels in IGCC. The field test performed in the IGCC pilot plant has demonstrated the combustor feasibility of achieving the dry low NO_x and flashback-resistant combustion for practical plants.

This paper also described applications of this combustion technology to DME and combustion with humidified and high-temperature air for fuel flexibility. The combustor has been extensively developed for a wide variety of fuels in order to expand fuel flexibility.

REFERENCES

- Abe, K., and Koganezawa, T., 2013, "Combustion Characteristics of Cluster Nozzle Burners for a 40 MW Class Advanced Humid Air Turbine System," *Proceedings of the International Conference on Power Engineering-13 (ICOPE-13)*, Volume 1, pp. 496-501.
- Asai, T., Koizumi, H., Dodo, S., Takahashi, H., Yoshida, S., and Inoue, H., 2010, "Applicability of a Multiple-Injection Burner to Dry Low-NO_x Combustion of Hydrogen-Rich Fuels," *Proceedings of ASME Turbo Expo 2010*, ASME Paper No. GT2010-22286.
- Asai, T., Dodo, S., Koizumi, H., Takahashi, H., Yoshida, S., and Inoue, H., 2011, "Effects of Multiple-Injection-Burner Configurations on Combustion Characteristics for Dry Low-NO_x Combustion of Hydrogen-Rich Fuels," *Proceedings of ASME Turbo Expo 2011*, ASME Paper No. GT2011-45295.
- Asai, T., Dodo, S., Akiyama, Y., Hayashi, A., Karishuku, M., and Yoshida, S., 2013, "A Dry Low-NO_x Gas-Turbine Combustor with Multiple-Injection Burners for Hydrogen-Rich Syngas Fuel: Testing and Evaluation of its Performance in an IGCC Pilot Plant," *Proceedings of ASME 2013 Power Conference*, ASME Paper No. Power2013-98122.



- Asai, T., Dodo, S., Karishuku, M., Yagi, N., Akiyama, Y., and Hayashi, A., 2015a, “Performance of Multiple-Injection Dry Low-NO_x Combustors on Hydrogen-Rich Syngas Fuel in an IGCC Pilot Plant,” *Journal of Engineering for Gas Turbines and Power*, 137(9), pp. 091504-1–091504-11.
- Asai, T., Dodo, S., Karishuku, M., Yagi, N., Akiyama, Y., and Hayashi, A., 2015b, “Part Load Operation of a Multiple-Injection Dry Low NO_x Combustor on Hydrogen-Rich Syngas Fuel in an IGCC Pilot Plant,” *Proceedings of ASME Turbo Expo 2015*, ASME Paper No. GT2015-42312.
- Dodo, S., Asai, T., Koizumi, H., Takahashi, H., Yoshida, S., and Inoue, H., 2013, “Performance of a Multiple-Injection Dry Low NO_x Combustor with Hydrogen-Rich Syngas Fuels,” *Journal of Engineering for Gas Turbines and Power*, 135(1), pp.011501-1–011501-7.
- Dodo, S., Karishuku, M., Yagi, N., Asai, T., and Akiyama, Y., 2015, “Dry Low-NO_x Combustion Technology for Novel Clean Coal Power Generation Aiming at the Realization of a Low Carbon Society,” *Mitsubishi Heavy Industries Technical Review*, 52(2), pp. 24-31.
- Higuchi, S., Koganezawa, T., Horiuchi, Y., Araki, H., Shibata, T., and Marushima, S., 2008, “Test Results From the Advanced Humid Air Turbine System Pilot Plant: Part 1–Overall Performance,” *Proceedings of ASME Turbo Expo 2008*, ASME Paper No. GT2008-51072.
- Kimura, N., 2005, “EAGLE Project – Perspective on Coal Utilization Technology,” *APEC Clean Fossil Energy Technical and Policy Seminar*.
- Kobayashi, N., Inoue, H., Koizumi, H., and Watanabe, T., 2003, “Robust Design of the Coaxial Jet Cluster Nozzle Burner for DME (Dimethyl Ether) Fuel,” *Proceedings of ASME Turbo Expo 2003*, ASME Paper No. GT2003-38410.
- Koganezawa, T., Miura, K., Saito, T., Abe, K., and Inoue, H., 2007, “Full Scale Testing of a Cluster Nozzle Burner for the Advanced Humid Air Turbine,” *Proceedings of ASME Turbo Expo 2007*, ASME Paper No. GT2007-27737.
- Lieuwen, T., 2012, *Unsteady Combustor Physics*, New York, NY: Cambridge University Press.
- Lieuwen, T., and Yang, V., 2005, *Combustion Instabilities in Gas Turbine Engines: Operational Experience, Fundamental Mechanisms, and Modeling (Progress in Astronautics and Aeronautics 210)*, Reston, Virginia, USA: American Institute of Aeronautics and Astronautics.
- Lieuwen, T., Yang, V., and Yetter, R., 2009, *Synthesis Gas Combustion: Fundamentals and Applications*, Boca Raton, FL: CRC Press.
- Murota, T., 2003, “A Dynamic Subgrid Scale Model of Eddy Viscosity Type Deduced from a Local Inter-Scale Equilibrium Assumption of Energy Transfer,” *Proceedings of Third International Symposium on Turbulence and Shear Flow Phenomena*, Volume I, pp. 425-430.
- Nagasaki, N., and Akiyama, T., 2014, “Special Issue: 5. State-of-the-Art Coal-Fired Thermal Power, 2. Integrated coal Gasification Combined Cycle, 2. Oxygen Blown,” *The Thermal and Nuclear Power Journal*, 65(10), pp. 759-763 (in Japanese).
- Nagasaki, N., Takeda, Y., Akiyama, T., and Kumagai, T., 2010, “Progress toward Commercializing New Technologies for Coal Use – Oxygen-Blown IGCC+CCS,” *Hitachi Review*, 59(3), pp. 77-82.
- Nagasaki, N., Sasaki, K., Suzuki, T., Dodo, S., and Nagaremore, F., 2013, “Near-Zero-Emission IGCC Power Plant Technology,” *Hitachi Review*, 62(1), pp. 39-47.
- Omata, K., 2014, “Oxygen-blown Coal Gasification System,” *Journal of the Japan Institute of Energy*, 93(7), pp. 624-630 (in Japanese).



45TH TURBOMACHINERY & 32ND PUMP SYMPOSIA
HOUSTON, TEXAS | SEPTEMBER 12 – 15, 2016
GEORGE R. BROWN CONVENTION CENTER

Saitou, T., Inoue, H., Kobayashi, N., and Watanabe, T., 2004, "Development of Multi-Cluster Burner for Fuel Grade DME," *Proceedings of ASME Turbo Expo 2004*, ASME Paper No. GT2004-53689.

Saitou, T., Miura, K., Inoue, H., Kobayashi, N., and Suzuki, S., 2005, "Performance Demonstration of the Full Size Multi-Cluster Combustor for DME under Real Engine Conditions," *Proceedings of ASME Turbo Expo 2005*, ASME Paper No. GT2005-68647.

Yunoki, K., Murota, T., Miura, K., and Okazaki, T., 2013, "A Numerical Simulation of Turbulent Combustion Flows for Coaxial Jet Cluster Burner," *Proceedings of ASME 2013 Power Conference*, ASME Paper No. POWER2013-98143.

ACKNOWLEDGEMENTS

The multi-cluster combustors for the IGCC have been developed under the "Innovative Zero-Emission Coal Gasification Power Generation Project: Development of Low NO_x Combustion Technology for High-Hydrogen Syngas in IGCC" by the New Energy and Industrial Technology Development Organization (NEDO) of Japan. The tests in the EAGLE plant were performed with the support of the Wakamatsu Research Institute of Electric Power Development Co., Ltd. (J-POWER). The combustor development has been performed with the support of the OSAKI CoolGen Corporation. The authors sincerely appreciate their valuable guidance and support.

The multi-cluster combustors for the AHAT system have been developed under the project by the Agency for Natural Resources and Energy, the Ministry of Economy, Trade and Industry (METI) of Japan. The authors sincerely appreciate their valuable guidance and support.

The multi-cluster combustors for DME have been developed under the project by the Japan Oil, Gas and Metals National Corporation (JOGMEC). The authors sincerely appreciate their valuable guidance and support.

This paper includes the American Society of Mechanical Engineers (ASME) copyrighted materials. The authors sincerely appreciate ASME's granting permission to use them in this paper. This paper also includes the materials in the proceedings of the International Conference on Power Engineering-13 (ICOPE-13) organized by Chinese Society of Power Engineering (CSPE). The authors sincerely appreciate their cooperation in this paper.